# UNIVERSIDAD CARLOS III DE MADRID

## Escuela Politécnica Superior

Departamento de Ingeniería de Sistemas y Automática



# Control de la forma de una superficie mediante SMAs

## Surface Morphing Using SMAs

**TRABAJO FIN DE GRADO**

**GRADO EN INGENIERÍA ELECTRÓNICA INDUSTRIAL Y AUTOMÁTICA**


Autor: Irene Álvarez Caro

Tutor: Dr. Luis Enrique Moreno Lorente



Septiembre 2014

# Resumen

En este proyecto se desarrolla el diseño, construcción y control de una superficie deformable por medio de hilos de Shape Memory Alloys (SMAs). Para ello primero se estudiará el estado del arte de los SMA, incluyendo su principio de funcionamiento, y el estado del arte de las superficies deformables.

Posteriormente se realizará un análisis de especificaciones y condicionantes para realizar el diseño de la superficie. En este aspecto, se tendrá en cuenta que una de las posibles aplicaciones futuras sería la realización de una superficie anti-escaras. Una vez realizado el diseño por ordenador con Autodesk Inventor de las distintas partes del prototipo, se pasará a la construcción de la maqueta. Al mismo tiempo se realizará el diseño de una placa de circuito impreso mediante OrCAD para los drivers que alimentan los actuadores de SMA. Una vez finalizado el diseño de la placa, se procederá al conexionado de la electrónica de control y potencia con el prototipo para poder así realizar su control y una serie de medidas experimentales con las que se podrá analizar el funcionamiento de la superficie.

Además durante el proyecto se utilizarán métodos de prototipado rápido como son la impresión 3D o la programación mediante bloques, que se obtiene con la herramienta Simulink de Matlab.

Por último se realizará un análisis completo del proyecto, así como de los resultados, y se estudiarán los posibles proyectos a desarrollar basándose en este.

# Palabras clave:

Actuador de SMA, superficie deformable, control en posición, escaras, impresión 3D, prototipado de control rápido

# Abstract

This project develops the design, assembly and control of a surface morphing using Shape Memory Alloy (SMA) wires. For this purpose, initially a study of art will be performed about SMA actuators, including its working principle, and about surface morphing.

Subsequently, specifications and constraints that would affect the surface design will be analyzed. In this regard, it will be considered that one of the possible applications of this project would be to develop an anti-bedsores surface. Once the computer design of the different components of the prototype is realized using Autodesk Inventor, the model will be assembled. At the same time, it will be design a printed circuit board using OrCAD for the drivers board that power the SMA actuators. Once finalized designing the board, the control and power electronics will be connected to proceed with the control adjustments and a series of tests will be run to evaluate the surface behavior.

In addition, during this project fast prototyping methods will be use as 3D printing or block programming through Simulink tool from Matlab.

Last, it will be analyzed the complete project, as well as the results obtained with the experimental tests. Also future projects that can be developed based on this project will be studied.

# Keywords:

SMA actuator, Surface morphing, Position control, Bedsores, Pressure Ulcers, 3D printing, Rapid control prototyping

# Acknowledges

I would like to acknowledge the people that have helped me during the development of this project. Specially, I would like to acknowledge the following people:

- My tutor, Luis Moreno, for propose me this project, for guiding and helping me during the project. This project has given me many opportunities to learn that I have not had during classes.
- Antonio Flores, Dorin Copaci and Alvaro Villoslada for helping me with the PCB, the control and 3D printing, and for their interest on the project.
- The laboratory technicians, Fernando and Angela, for helping me in my process of self-learning to use OrCAD, I do not think I could have finished the PCB without the time they spent in helping me

I would also like to acknowledge the people that helped me to decide to study engineering. Specially, I would like to acknowledge the following people:

- Joseph Vanderway for giving me the opportunity to be part of Robodox, for pushing me beyond what I thought was my limit and for showing me that engineering was not what I thought. I would not be doing this project if he had not given me that opportunity.
- Chris Siegert for supporting me all these years, for getting me to like programming and for not allowing me to settle with good but to aim for great.
- Andrew Freesh for constantly giving me opportunities to learn, for letting me build stuff and for being always there when I need him.
- Robodox for being a family and for changing the career I wanted to pursue.
- Juan Carlos Hernández for giving me the opportunity to build my first robot and for helping me to decide to study at the UC3M.

I would like to acknowledge my parents for allowing me to follow my dreams and for giving me what you thought was the best.

Last, I would like to acknowledge the people that all this years have told me that I was not going to make it, that I should not study engineering, that I should not pursued what I wanted… all those things have made me pursue my goals harder.

# Table of Contents

# Table of Figures

# Table of Tables

# 1. Motivation

Due to the Industrial Revolution, an later the creation of the first powered vehicles, the number of accidents with spinal cord injury increased. These injuries cause the person to live with reduce mobility which can meant the person to have to stay in bed or to move with help of a wheelchair, also some diseases cause to temporal or permanent reduced mobility. These cases of reduced mobility can lead to other injures as pressure ulcers. [28]

Pressure ulcers, bedsores, are the result from prolonged pressure on the skin, and they are more common on areas in which skin is covering a bone, fig. 1. These are difficult to treat and can present other complications like sepsis, cellulitis, bone and joint infections and cancer. In addition to the treatment provided to heal any wound, both to prevent and to promote healing practices of repositioning and using support surfaces are used. [24][25]

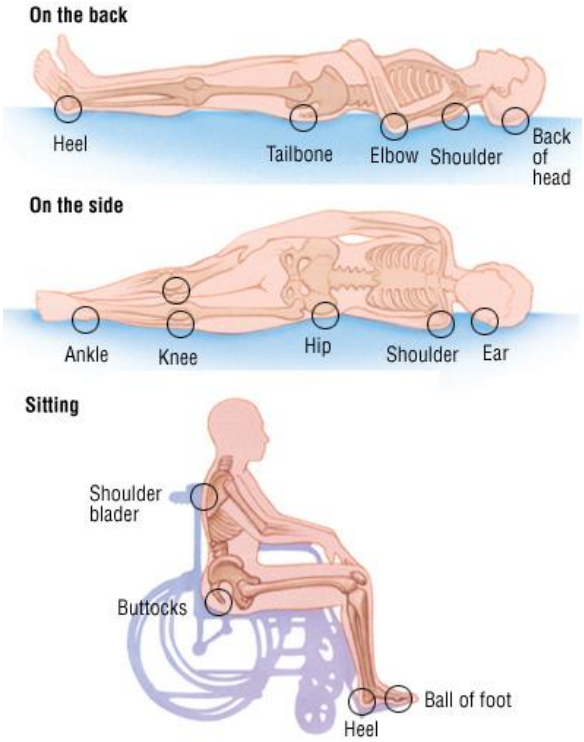


**Figure 1: Areas on Which Bedsores Appear More Frequently [24]**

Common medicine practice advocate to develop mechanisms that ease repositioning as in some cases this can be difficult to achieve due to the frequency and need of another person for repositioning. This prevention was first achieved with help cushions that were designed to decrease pressure on specific points which was achieve with silicon and air cells integrated on foam cushions. Later, air mats were developed

to change pressure points with compressed air, but the need of a compressor or the use in other mats of motors produce a high amount of noise. On the other hand, SMA actuators do not emit any noise, which makes them ideal candidates for the development of a morphing surface intended for therapeutic purposes. This concept will be the main focus of this project.

# 2. Goals and Regulatory Framework

This project pursued to develop a surface morphing using shape memory alloys (SMA) that could be applied in a future work to prevent bedsores. To achieve this goal a series of different objective were set. The first objective was to realize a study of the state of art of SMA actuators and morphing of surfaces. The purpose of this was to know the limitations of SMA actuators and different approaches that have been made to develop smart surface that can be controlled.

Next objective was to design a model of a surface that could adapt to different shapes and which would be actuated by SMA using Matlab. To achieve this, first, the surface should be designed and built using 3D printers for a fast prototyping and later SMA wires and its electronics should be connected to the surface.

The third objective would be to control the surface developed using the Simulink suite from Matlab. This would be done by adapting the SMA position and velocity controller developed in the University Carlos III of Madrid so the controller can react correctly to the changes produced on the surface.

Finally the surface model will be tested to analyze the results and conclude the viability of developing an anti-bedsores' surface. Also it will be analyzed the improvements that could be realized on the project and future projects that could be developed based on this one.

Because of these goals during the project no regulation will applied and depending on the future works developed different regulations will need to be studied as could be medical regulations, in the case of an anti-bedsore surface, or military regulations, in the case of applying the surface in a military field.

# 3. Planning

Before starting the project, a Gantt planning and analysis was realized to organize the project and to track the progress of it. Before creating the Gantt chart the project itself was analyzed to identify essential tasks and task's relationships, in this project also subtasks were identify as some of the essential tasks considered were broad tasks.

- **Essential Tasks**

Instead of noting its earliest start date while identifying the essential task, as this will be affected by task relationships, tasks were noted by priority. Initially the essential tasks identified were:

**Table 1: Essential Tasks**

| Priority | Task | Estimated time |
|---|---|---|
| 1 | Bibliography compilation | 1 month |
| 2 | Study of the state of art | 1 month |
| 3 | Mechanical prototype | 4 months |
| 3.1 | Prototype's design | 3 months |
| 3.2 | Prototype's assembly | 1 month |
| 4 | Surface control | 1 month |
| 5 | Experimental measurements | 1 month |
| 6 | Thesis writing | 3 months |

- **Task's Relationships**

**Table 2: Task's Relationships**

| Task | Dependences |
|---|---|
| Bibliography compilation | - |
| Study of the state of art | To finish bibliography compilation |
| Mechanical prototype | Finished study of the state of art |
| Prototype's design | Started mechanical prototype |
| Prototype's assembly | Finished prototype's design |
| Surface control | Finished mechanical prototype |
| Experimental measurements | Started surface control |
| Thesis writing | Finished study of the state of art |

Even though thesis writing it could be realized parallel to other task; it was planned since the beginning to be realized after experimental measurements in order to combine this project with academic course and a part time job.

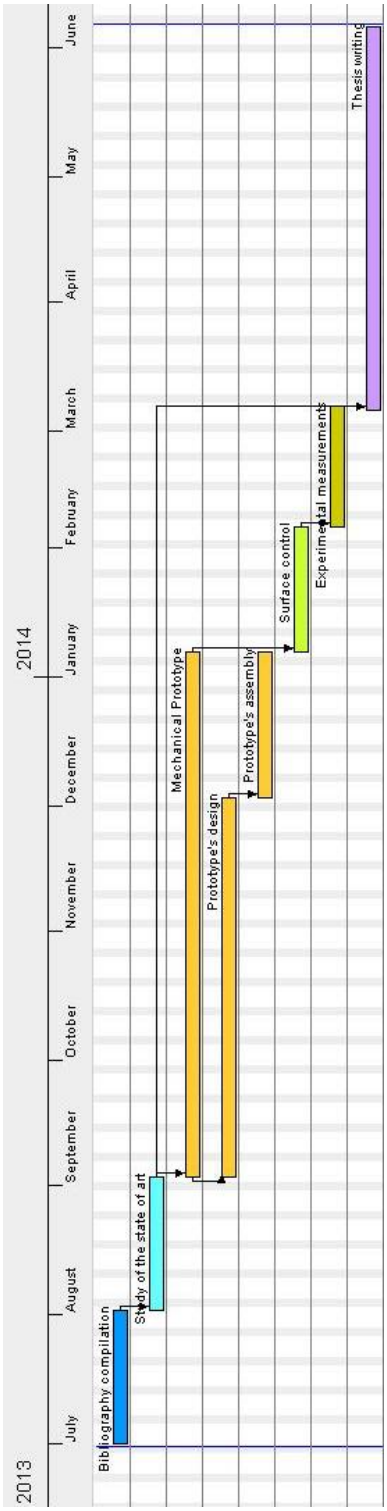


**Figure 2: Planned Gantt's Diagram**

While developing the project and due to the number of SMA actuators needed, it was needed to include a new task to develop a printed circuit board for the SMA drivers, this new task modified the Gantt's diagram as it can be observed on fig. 3.

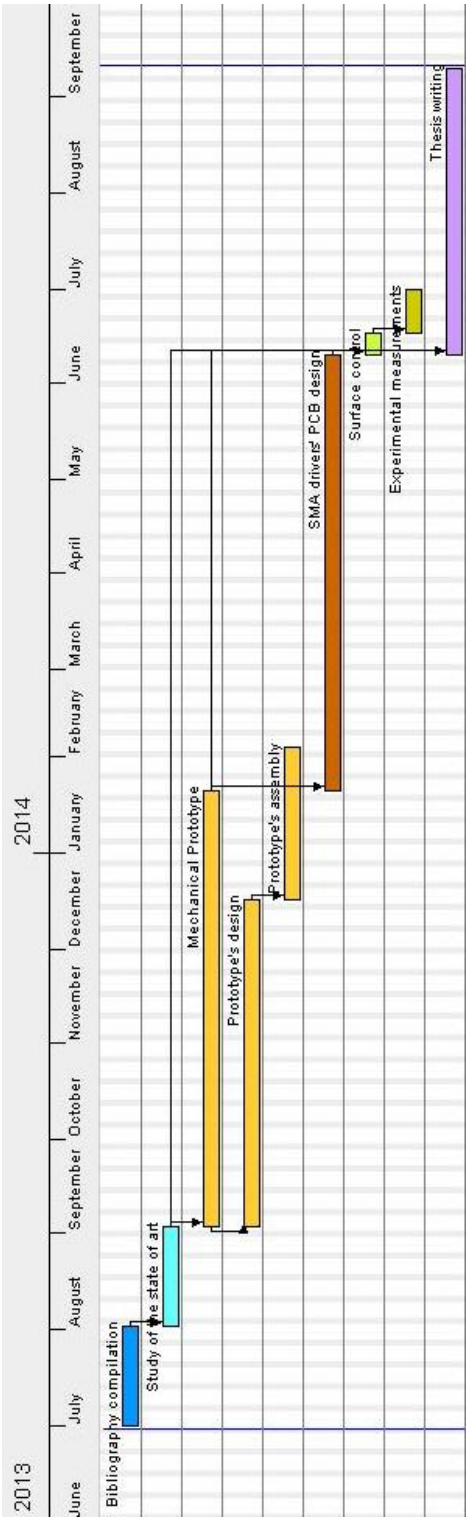


**Figure 3: Real Gantt's Diagram**

# 4. State of art

## 4.1. Shape Memory Alloys SMA

In this project I have used shape memory alloys (SMA) which are a kind of metallic alloy that show a shape memory effect and superelasticity. These characteristics allow using SMA as a mechanical actuator, which process is explained in the following sections.

### 4.1.1. History of SMA

The first shape memory alloy was discovered on 1932 by Arne Olander in an Au-Cd alloy in which he observed a shape and recovery ability. This ability allow to deform plastically in cool and when heated it would recover its original shape. Olander observed two different phases of Au-Cd, austenite and martensite, which were involved in the shape memory effect. A few years after, in 1938, Greninger and Mooradian noted this effect in Cu-Zn and Cu-Sn alloys. In 1958, Chang and Read performed an X-ray investigation to analyze the changes in electrical resistivity and the orientation on the particles. Also, they were able to record the movements of the particles during the change of phases and they show that SMA could be used to perform mechanical work by lift weights. However until the 1960s researchers had not being interested on developing applications using SMA, one of the events that produced this shift was in 1961 when the group led by Beuhler at the U.S. Naval Ordnance Laboratory discovered that the alloy formed by nickel and titanium (Ni-Ti) exhibit the shape memory effect. The alloy was named Nitinol in reference to the Naval Ordnance Laboratory. Nitinol is less expensive, easier to work with and less hazardous to health than the previously discovered SMA.[2][3]

The first application of SMA was developed in 1971 by Raychem in which he used a Ni-Ti-Fe coupling to connect titanium hydraulic tubing in the Grumman F-14 aircraft [5]. After that, in 1975 Andreasen used SMA for an orthodontic implant making use of the superelasticity properties that SMA exhibit [2]. In other fields, researchers started to develop applications in which they would use SMA as an actuator, for example the company Delta Metal suggested using SMA to control greenhouse windows, valves that regulate building temperatures and automobile fan clutches; this was possible because SMAs must suffer a cycle of heating, cooling and deformation to perform mechanical work. In 1971, Sawyer and his coworkers developed and tested an artificial heart using SMA to produce the contraction, fig. 4 [17]. In 1982, Sharp started using

SMA actuators for oven dampers and, in 1983, Matsushita Electric developed air conditioners with SMA actuated louvers. [3]

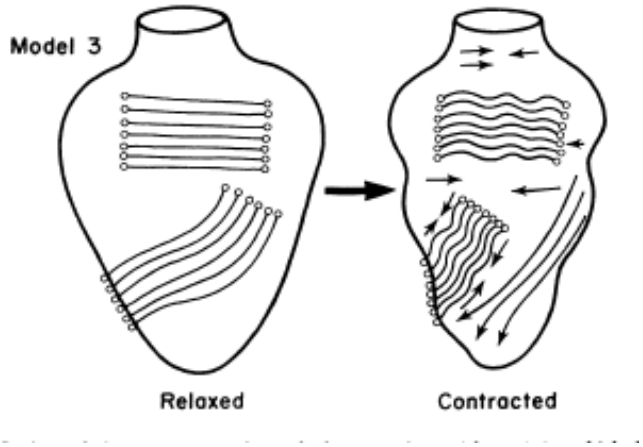


**Figure 4: Swayer's Artificial Heart Model [17]**

Other applications developed during the last years and the events that allow the shape memory effect and superelasticity are developed in the following sections.

### 4.1.2. Shape Memory Effect and Superelasticity

SMA wires can be considered as thermal actuators as they are capable of produce mechanical work by means of a heat source, this is achieved by the alteration of size that is produced on SMA ought to temperature change and which produce a force and displacement.

Its behavior is due to the change of phase from martensite to austenite when heating the alloy. When the material is heated sufficiently, grains form a rectangular crystalline net as austenite phase allow grains to rearrange. Once the material is cool the crystalline structure change to martensite in which the net is twinned, this produce that when the material is deform plastically in cool it becomes martensite de-twinned and when is reheated until austenite phase grains will arrange again forming the starting crystalline net. [3]

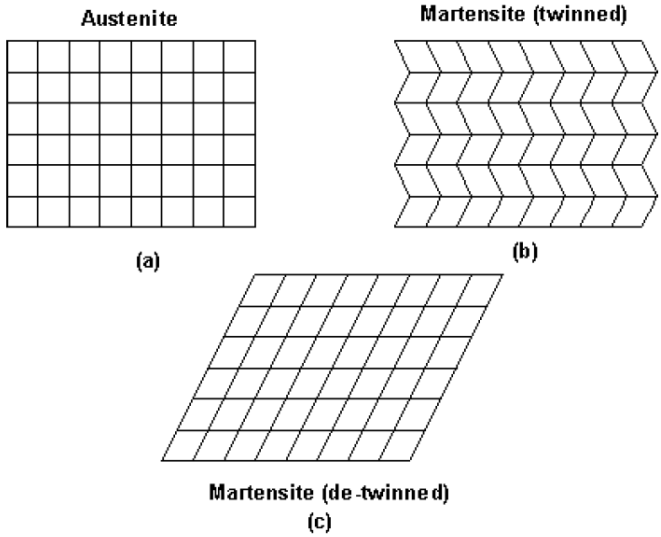


**Figure 5: Material Crystalline Arrangement During the Shape Memory Effect [3]**

As briefly introduced earlier shape memory and superelasticity effects have been discovered in several alloys: Ni-Ti, Ag-Cd, Cu-Al-Ni, Cu-Zn-(X), In-Ti, Ni-Al, Fe-Pt, Mn-Cu and Fe-Mn-Si among others. Among the different alloys, Ni-Ti has proved to be the most flexible and beneficial alloy to engineer different applications due to the following characteristics that exhibits: corrosion resistance, great ductility, bigger recoverable movement range, stable transformation at high temperatures, high biocompatibility and the ability to be electrically heated. [3]

**Table 3: High Temperature SMA (HTSMA) Groups and their Properties [1]**

| Group | Alloy composition | Transformation temperature range (°C) | Thermal hysteresis (°C) | Strain (%) | Recovery (%) |
|---|---|---|---|---|---|
| 100-400°C | Ti-Ni-Pd | 100-530 | 20-26 | 2.6-5.4 | 90-100 |
| | Ti-Ni-Pt | 110-1100 | 31-55 | 3-4 | 100 |
| | Ni-Ti-Hf | 100-400 | 60 | 3 | 100 |
| | Ni-Ti-Zr | 100-250 | 54 | 1.8 | 100 |
| | Cu-Al-Ni | 100-400 | 21.5 | 3-5 | 80-90 |
| | Cu-Al-Nb | 100-400 | 59-170 | 5.5-7.6 | - |
| | Co-Al | 100-400 | 121 | 2 | 90 |
| | Co-Ni-Al | 100-400 | 15.5 | 5 | 100 |
| | Ni-Al | 100-300 | - | - | - |
| | Ni-Mn | 100-670 | 20 | 3.9 | 90 |
| | Ni-Mn-Ga | 100-400 | 85 | 10 | 70 |
| | Zr-Cu | 100-600 | 70 | 8 | 44 |
| | Ti-Nb | 100-200 | 50 | 2-3 | 97-100 |
| | U-Nb | 100-200 | 35 | 7 | 97-100 |
| 400-700°C | Ti-Pd | 100-510 | 40 | 10 | 88 |
| | Ti-Au | 100-630 | 35 | 3 | 100 |
| >700°C | Ti-Pt-Ir | 990-1184 | 66.5 | 10 | 40 |
| | Ta-Ru | 900-1150 | 20 | 4 | 50 |
| | Nb-Ru | 425-900 | 20 | 4.2 | 88 |

Shape memory alloys can be classified under the shape memory effects that it shows. There are three categories:

- **One Way Shape Memory Effect (OWSME):** deformation produced by an external force is maintained and it recovers its original shape after heating. It has been discovered that this effect is also present in no metallic materials as polymers and ceramics. [1][4]

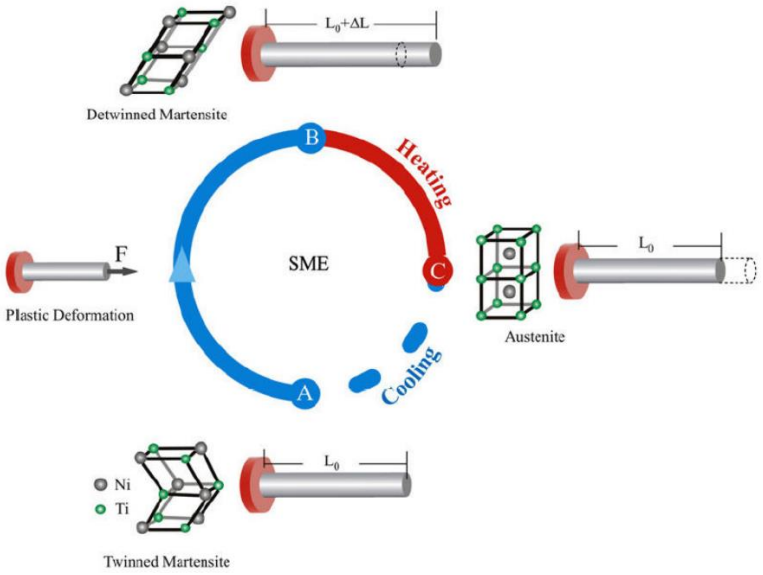


**Figure 6: One Way Shape Memory Effect Cycle [4]**

**Table 4: Materials with SME [1]**

| Materials | Examples |
|---|---|
| Metals | • Ni-Ti based alloys: Ni-Ti, Ni-Ti-Cu, Ni-Ti-Pd, Ni-Ti-Fe, Ni-Ti-Nb…<br>• Cu based alloys: Cu-Zn, Cu-Zn-Al, Cu-Al-Ni, Cu-Sn, Cu-Al-Ni-Mn…<br>• Ag based alloys: Ag-Cd<br>• Au based alloys: Au-Cd<br>• Co based alloys: Co-Ni-Al |
| Polymers | PTFE, PU, Poly-caprolactone, EVA + nitrile rubber, PE, Poly-cycliictene, PCO-CPE blend, PLC-BA copolymer, PET-PEG… |
| Ceramics | $ZrO_2$ $(PSZ)$, MgO, $CeO_2$, PLZT, PNZST… |

- **Two Way Shape Memory Effect (TWSME):** in this case the SMA not only remembers the shape of the austenitic phase but it also remembers the shape of the martensitic phase. This effect produces that material shape can be modified between two different phases by applying different temperatures between the martensitic and austenitic phases. However the

stress produced is about half of the produced by OWSME and the material deteriorates faster. [1][4]

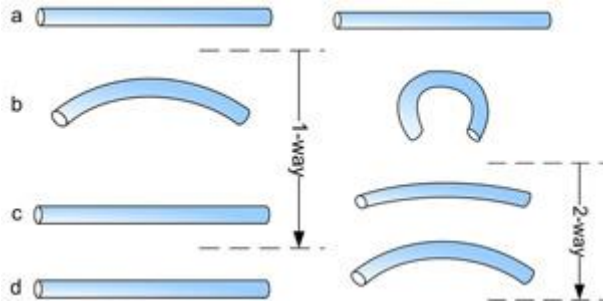


**Figure 7: TWSME Compared With OWSME (a: Martensite; b: Severe Deformation (With an Irreversible Amount at the TWSME); c: Heated; d: Cooled) [23]**

- **Superelastic Effect (SE):** this behavior appears when we apply a load on the material while it is at the austenitic phase. As it has been explained before when a load is applied to the SMA, it deforms and the crystalline structure change to martensite de-twinned, this phase is unstable at high temperatures, therefore when the SMA is unloaded it returns to austenite and recovers its original shape. [1][4]

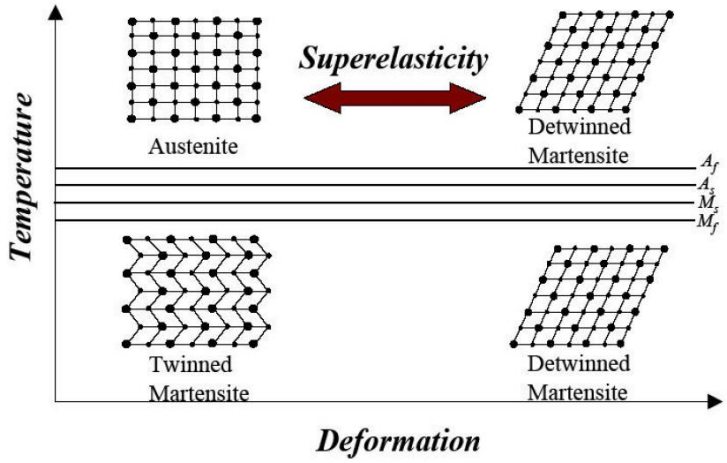


**Figure 8: Superelastic Effect Representation [4]**

Most applications are based on the OWSME due to disadvantages annotated earlier for the TWSME actuators. For that reason it will only be considered the one way shape memory effect while talking about SMA wires, where the temperature rise produces a contraction of the wire. In this direction, three different types of actuators can be distinguished:

- **One-way Actuator (fig. 9a):** once the SMA wire is heated it pulls the element P to the left. [15]

- **Biased Actuator (fig. 9b):** by using, for example, a spring it can be achieved that the element P recovers its initial position while is controlled by a single SMA wire. [15]

- **Two-way Actuator (fig. 9c):** in this actuator, as in the previous case it can be achieved a controlled movement in both directions of the element P by using two wires of SMA in opposed positions that are heated and cooled alternately. [15]

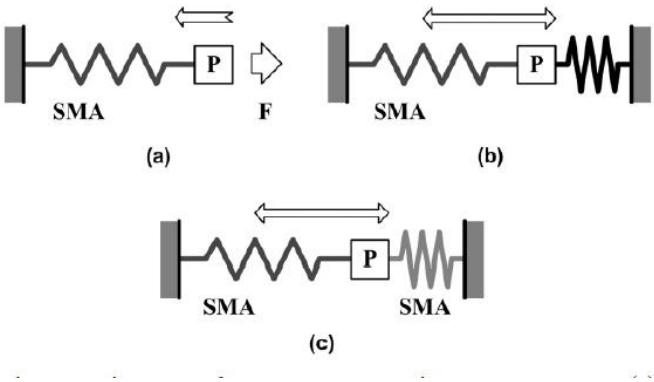


**Figure 9: Basic Types of SMA Actuators using One Way SMA [15]**

To heat the SMA wires, mainly three different methods are used:

- Passing an electric current through the wire, this method can only be used with SMA wires or springs with a small diameter. [15]

- Passing an electric current through a resistive wire wound it round the SMA piece. [15]

- By means of hot water or air, or exposing the material to thermal radiation. [15]

When SMA actuators are used it has be taken into account the cooling speed effect and to study the need of using external methods to increase that velocity.

### 4.1.3. SMA Applications

Because of the exposed characteristics, during the last years different applications have been developed in several areas using SMA. In the following paragraphs some of the most outstanding applications in automobiles, aeronautics, robotics and biomedicine will be described.

In the automobile industry the first car introducing a SMA actuator was the Chevrolet Corvette that implemented a system to facilitate closing the trunk. Other applications that have also being implemented are: a system to protect pedestrians, actuators for lateral driving mirrors, a micro-scanner to measure distance and angle to objects, powertrain clutches, valves… [1]

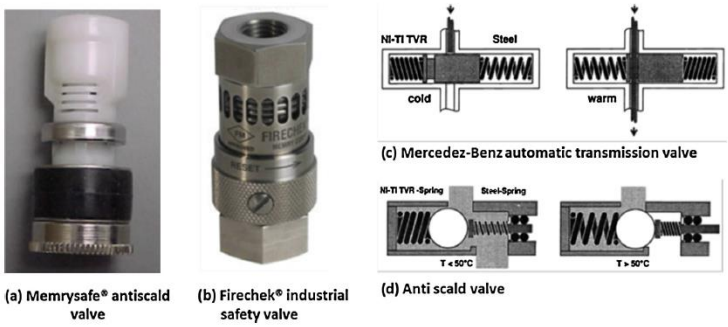


**Figure 10: Ni-Ti Thermovariable Rate (TVR) Springs Applications [1]**

Furthermore mentioned applications that have been implemented, other applications have been suggested and even patented but it has not being possible to develop technologically or economically. One of these applications is using SMA in batteries, this is being researched by Leary et al. [1]

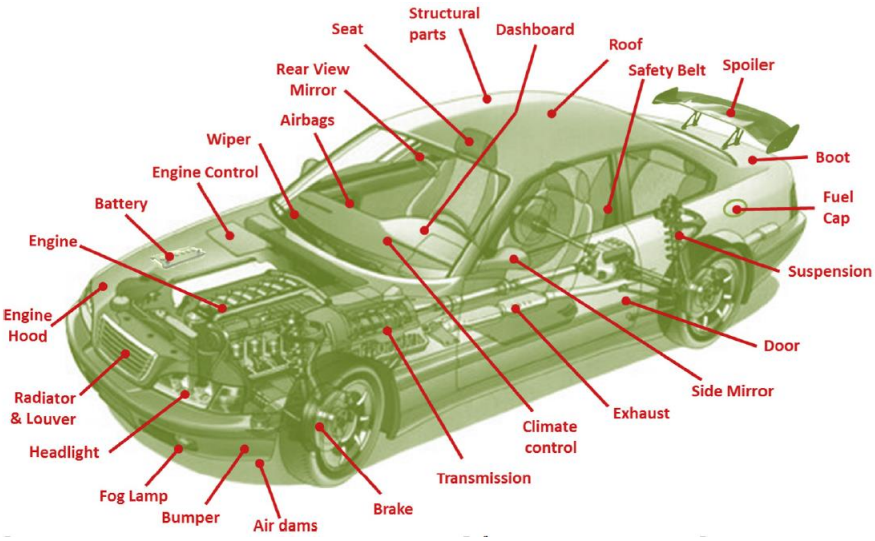


**Figure 11: Existing and Potential SMA Applications in the Automotive Domain [1]**

The benefit of using NiTi SMA in automobile's field is that it operates in the range of temperatures at which passengers can be exposed. [1]

The aeronautics industry first used SMA in 1970 at the hydraulic system of fighter planes. Subsequently in 1990 researchers focused on building active and adaptive structures following the tendency to create deformable actuated surfaces and consequently optimize different flight systems in planes for flight conditions. One of the noteworthy projects is developed by DARPA and it has being named “Smart Wings”, fig. 12. [1]

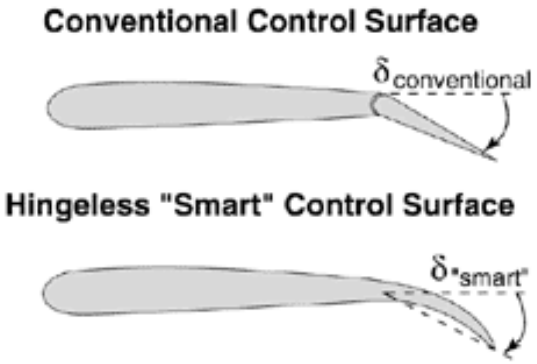


**Figure 12: Deflection Definitions Used for the Smart Wing Program [26]**

Particularly SMA has being used in space ships, for example in low-shock release mechanisms because they can be actuated gradually with heat, can absorb vibrations and can be fabricated in simple and compact designs, which is a necessity in this field. [1]

Other applications in the aeronautics industry with SMA are vibration absorption and isolation, telescopic wings systems, changes in the morphology of wings, retractable landing gear, components of the aircraft engine, change of morphology in structures… [1]

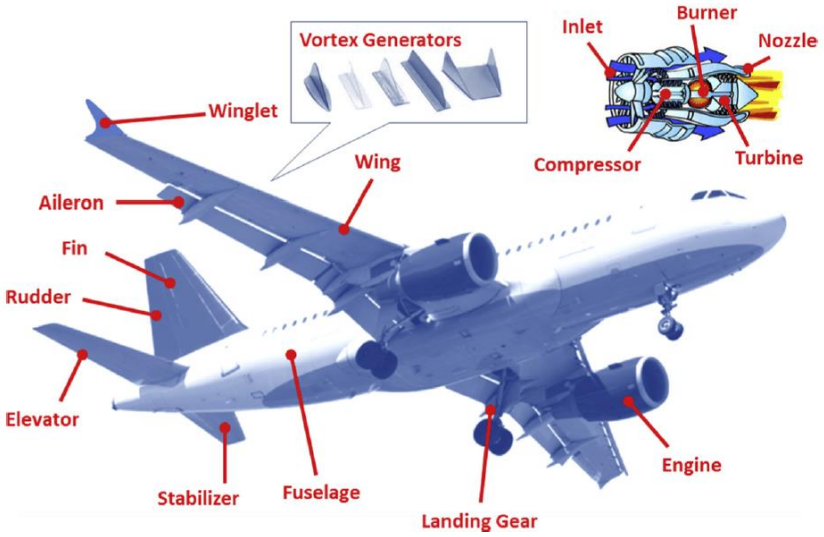


**Figure 13: Existing and Potential SMA Applications in the Aerospace Domain [1]**

SMA has also been used for robotics since the 80's, mainly as microactuators and artificial muscles which has been described by Furuya and Shimada, and Sreekumar et al. Nowadays, most of the applications are biomechanics applications; an example of this is a prosthetic hand developed by Chee Siong et al, in this model they used two SMA actuators by finger and they controlled with PWM pulses to avoid overheating, fig. 14. There are also other designs bio-inspired like a robotic fish devised by Tao et al. [1]

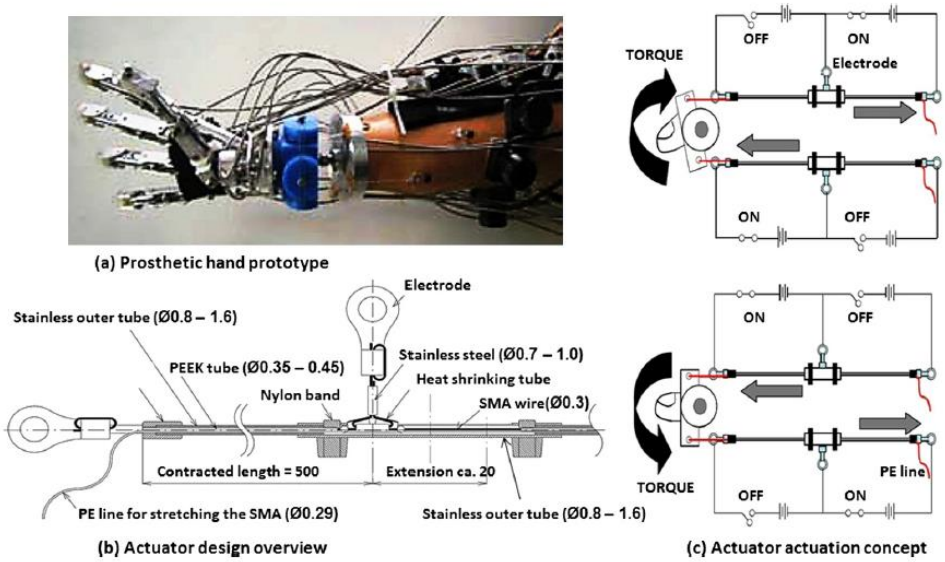


**Figure 14: Prosthetic Hand by Chee Siong et al [1]**

Other applications developed with SMA are passive micro-grippers that are controlled by magnetics fields and artificial rat whiskers which are used to navigate in small spaces and to locate micro-characteristics on surfaces. Also by means of SMA actuators, several flying robots have been devised as BATMAV and Bat Robot, in that field Festo group has developed a dragonfly, "BionicOpter", with a length of 44cm and a wingspan of 63 that use four SMA actuators to control some of its thirteen degrees of freedom, fig. 15. [1]

**Figure 15: Festo BionicOpter [1]**


**Figure 16: Existing and Potential SMA Applications in the Robotics Domain [1]**

In biomedicine SMA is used in numerous applications like orthodontic braces, stents, bone's implants, scoliosis correction… in addition to the robotics prosthetics that have been mentioned earlier. [1]

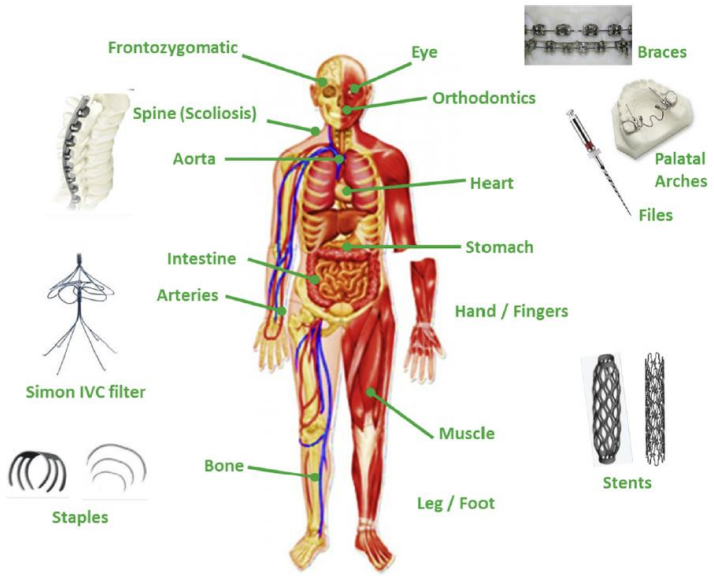


**Figure 17: Existing and Potential SMA Applications in the Biomedical Domain [1]**

One of the most common applications is its use for stents to keep a blood vessel straight as SMA is capable of resist blood flow and provide a small expansion force towards the vessel's walls avoiding these to block. Also, thanks to the superelasticity effect surgery risks are minimized as the stent is capable of adapting to closed angles. Another application is bone's implants with alterable stiffness as it has been discover that they improve and speed up healing; in this case heat induction is used to alter the Ni-Ti implant, fig. 18. [1]

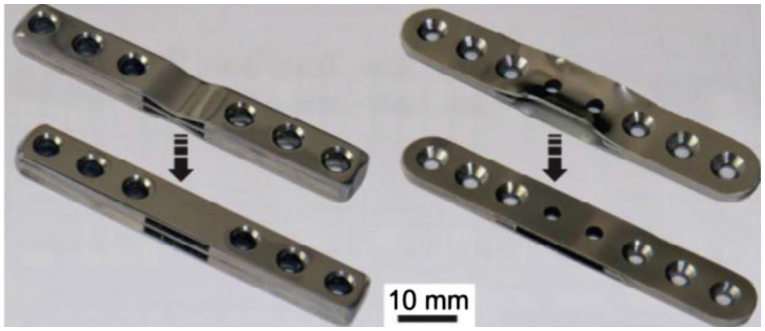


**Figure 18: An "Alterable Stiffness" Bone's Implant [1]**

With the discover of different materials that present shape memory effect like polymers or ceramics it is expected a development of more applications making use of these materials because of the advantages that they present. [1]

### 4.1.4. Nitinol

Nitinol is the SMA that will be use for the development of this project. Nitinol is an alloy form by Nickel and Titanium and is named in reference to the Naval Ordnance Laboratory which discovered this SMA in 1960. It is the SMA most used in engineering applications because it is the most flexible and beneficial for these due to its characteristics: corrosion resistance, great ductility and biocompatibility and ability to be electrically heated. Ni-Ti physical properties can be observed in table 5. [3]

**Table 5: Physical Properties of Ni-Ti [3]**

| Property | Austenite | Martensite |
|---|---|---|
| **Melting Temperature** ℃ | 1300 | |
| **Density,** $g/cm^3$ | 6.45 | |
| **Resistivity,** $\mu\Omega \cdot cm$ | Approx. 100 | Approx. 70 |
| **Thermal Conductivity,** $W℃/cm$ | 18 | 8.5 |
| **Corrosion Resistance** | Similar to 300 series stainless steel or titanium alloys | |
| **Young's Modulus, GPa** | Approx. 83 | Approx. 28 to 41 |
| **Yield Strength, MPa** | 195 to 690 | 70 to 140 |
| **Ultimate Tensile Strength, MPa** | 895 | |
| **Transformation Temperatures,** ℃ | -200 to 110 | |
| **Laten Heat of Transformation,** $KJ \cdot atom/kg$ | 167 | |
| **Shape Memory Strain** | 8.5% maximum | |

The properties on table 5 are modified by the composition of the alloy affecting mostly on the martensite start temperature (fig. 19) which also modify its temperature hysteresis loop.

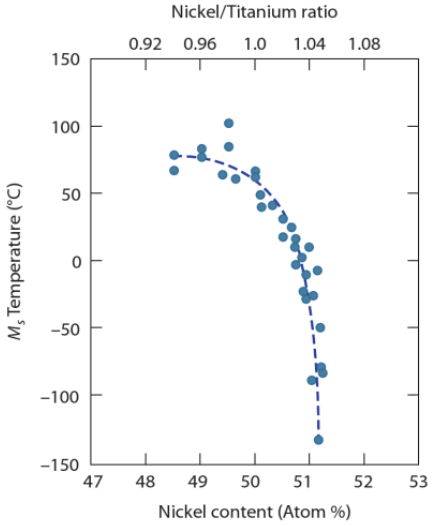


**Figure 19: Effect of Nitinol Composition on the Ms Temperature [27]**

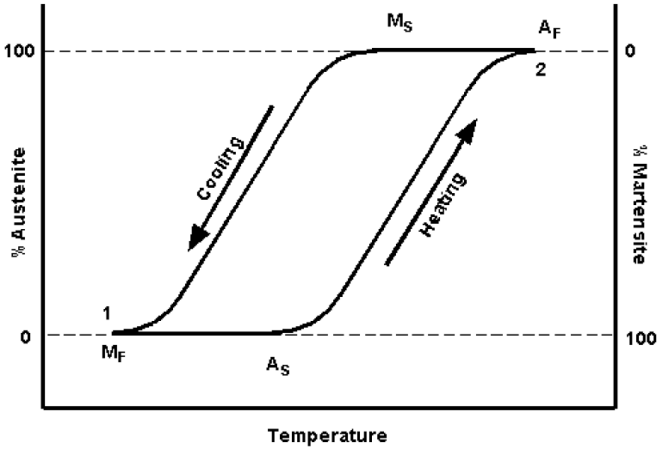


**Figure 20: Typical Temperature Hysteresis Loop in SMA [3]**

### 4.1.5. Advantages and Disadvantages

When an application using SMA actuators is implemented, all the advantages and disadvantages that it presents compered to classical actuators need to be considered. These can be observed in the following tables.

**Table 6: Comparison of Actuator Performance [1]**

| Actuator type | Stress (Mpa) | Strain (%) | Efficiency (%) | Bandwidth (Hz) | Work per Volume ($J/cm^3$) | Power per Volume ($W/cm^3$) |
|---|---|---|---|---|---|---|
| Ni-Ti SMA | 200 | 10 | 3 | 3 | 10 | 30 |
| Piezoceramic | 35 | 0.2 | 50 | 5000 | 0.035 | 175 |
| Single Crystal Piezoelectric | 300 | 1.7 | 90 | 5800 | 2.55 | 15,000 |
| Human Muscle | 0.007-0.8 | 1-100 | 35 | 2-173 | 0.035 | 0.35 |
| Hydraulic | 20 | 50 | 80 | 4 | 5 | 20 |
| Pheumatic | 0.7 | 50 | 90 | 20 | 0.175 | 3.5 |

**Table 7: Comparative Performances of Linear Actuators [18]**

| Technology | Force (N) | Voltage (V) | Stroke (mm) | Weight (g) | Volume ($cm^3$) | Peak Power (VA) | Avg. Power per cycle (W) | Response time (s) | Cost (€) |
|---|---|---|---|---|---|---|---|---|---|
| SMA | 100 | 12 | 10 | 240 | 357.5 | 1000 | 690 | 0.8 | 12 |
| Electromechanical | 37 | 12 | 10 | 700 | 660 | 100 | 84 | 0.5 | 10 |
| Pneumatic | 35 | | 12 | 170 | 294 | 110 | 60 | 0.5 | 8 |

As SMA actuators are mainly composed by a SMA wire its low weight and size benefit mechanical designs and reduce its complexity. Also force-weight ratio is much higher than classical actuators, for example a Ni-Ti actuator can apply until 600MPa. Moreover the behavior of these actuators can be considered biomimetic and compared with other actuators for the same force they have a lower cost. Another advantage is that is a noiseless actuator unlike conventional actuators, particularly pneumatic and hydraulic actuators. [3]

On the other hand, while designing a system with SMA actuators we have to bear in mind the cooling cycle that it is slower than the heating cycle, even though it can be accelerated using heat sinks, forced convection and liquid refrigerants. One more disadvantage is that the efficiency of this actuator is lower than others as it cannot be higher than the Carnot's cycle as the action principle is based on converting thermal energy in work, at regular working temperatures efficiency does not overpass 10%. Last, SMA actuators present hysteresis effects produced by temperature, deformation and heat transfer, therefor it is a nonlinear actuator which difficult its control. [3]

## 4.2. Deformable Surfaces

Nowadays most of the projects that use morphing surfaces are found in aeronautics where its usefulness is based on adapting an aircraft to different flight conditions as aircrafts are designed for ideal conditions. To perform these morphing multiple aerodynamic devices, as flaps and slats, are used but the problem is that this originates non continuous surfaces when ideal surfaces would be continuous and smooth morphology as birds present. The same need is found in anti-bedsores' surfaces, one of the possible applications on this project, were the human body needs a smooth surface morphing. [7]

In aeronautics, there have been several developments with morphing mainly to modify aircraft's span, sweep and camber of the wings. Since 1970s with the discovery of "smart" materials, as SMA, new projects have arisen with the goal of creating a continuous deformable controlled surface. To reduce complexity, what has been done is to embed active materials in the structure (fig. 21). [7]

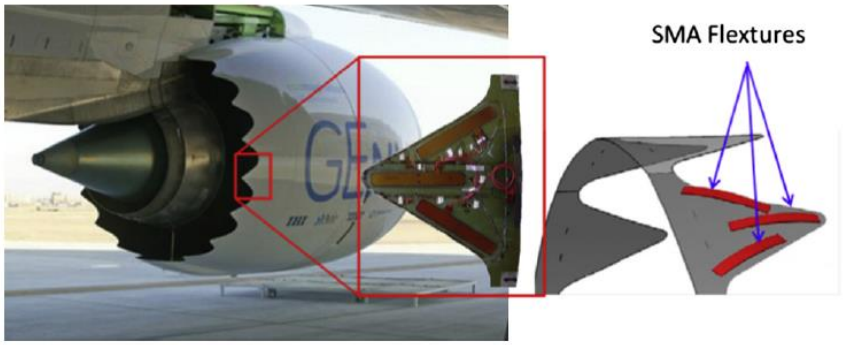


**Figure 21: Boeing's variable geometry chevron (VGC) [1]**

A different research with morphing surfaces has been conducted by MIT Tangible Media Group. They have developed a dynamic shape display, named inFORM, with the goal of allow users to interact with digital information in a tangible way. In this case, the surface is composed by square columns and is actuated with motors, by using push-pull rods to enable a dense pin arrangement. The system has a height of 1100mm and the deformable surface area is 381x381$mm^2$. In this case the resulted surface is non-continuous. [8]

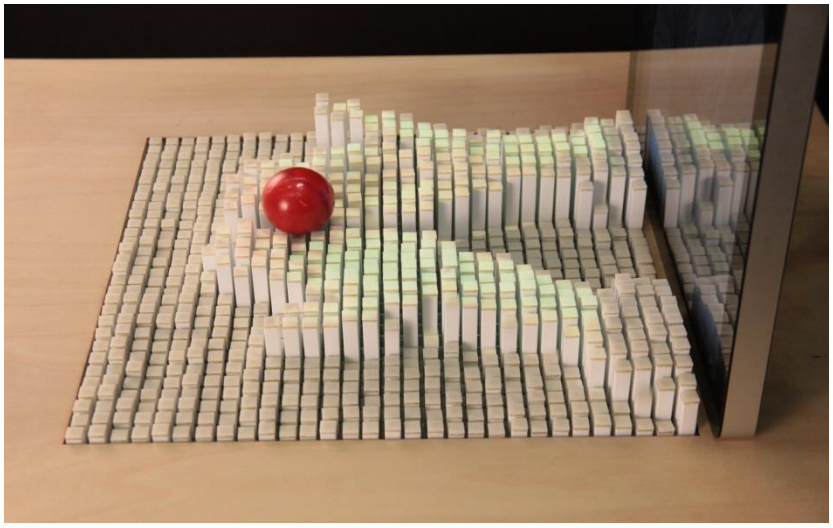

**Figure 22: InFORM Surface [8]**

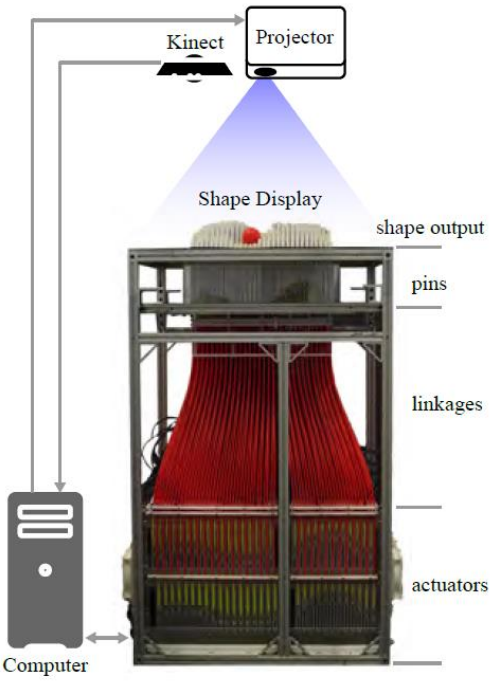


**Figure 23: The inFORM system schematic [8]**

In conclusion, actual researches focus on achieving morphing continuous surfaces to imitate biological systems that do not present discontinuities and that are especially adapted for specific tasks.

# 5. Prototype Design

This project was split in different parts that were developed a part and put together during the last stage of the project. These parts were mechanical design of the surface, SMA drivers PCB design, SMA position control and surface control. In the following sections is developed the design and implementation of each of the parts.

## 5.1. Mechanical Design

In this part the waterfall design process was used. This is a linear process in which the project moves from one phase to the following once the previous one is complete. It also focus on the analysis and critique of each phase to determine if is completed, as it is not is expected to go back to previous phase until the testing phase is achieved. [22]

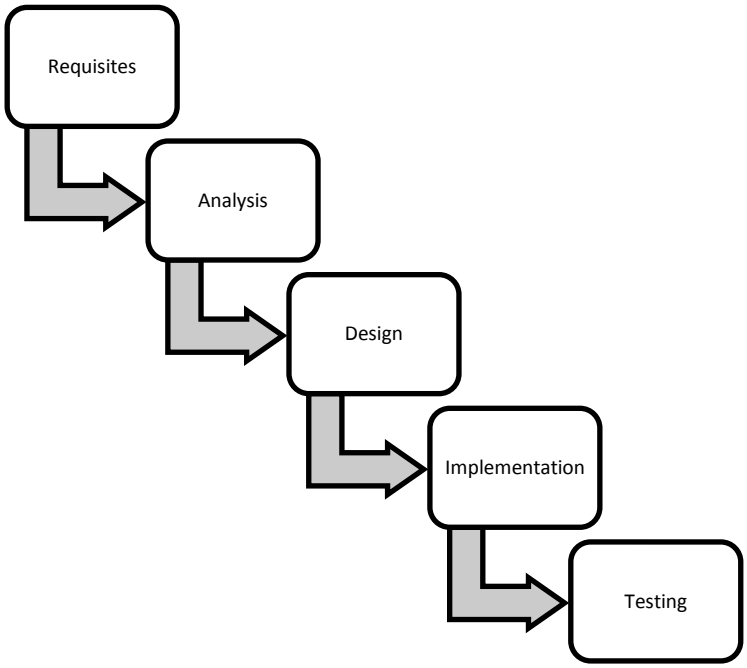


**Figure 24: Waterfall Design Process [22]**

Autodesk Inventor was used to design the project's prototype due to the access to a student software license and as it is one of the most common 3D CAD design tools, which provides a big community of users providing solutions and tutorials that eases the process of learning the use of a new tool.

### 5.1.1. Requisites

The idea of this project came from the need to study the possibility of developing an anti-bedsores' surface; therefore, some of the requisites came from this disease. The requisites evaluated were:

- To be a continuous surface
    - If it is not continuous:
        - To use rounded edges to avoid injuring the skin
        - To covert the whole surface with a fabric, which will help to smooth the surface and resemble a continuous surface
    - To have a dense amount of variation points to create smoother as possible surface
- To be actuated by SMA
    - To integrate a recovery mechanism when the SMA colds
- To measure movements of the surface

### 5.1.2. Analysis

In this phase I analyzed the different requisites to determine design constrictions that will be apply during the designing phase.

- To be a continuous surface

To be considered a continuous surface it could not be actuated point by point and it should be actuated globally. As SMA wires are going to be used, a possibility is to create a sheet by weaving SMA wires. Those wires have to be completely heat and electrically isolated and then the cooling cycle could be very slow. For this reason it is thought that a better solution could be a non-continuous surface actuated point by point.

- If it is not continuous:
    - To use rounded edges to avoid injuring the skin
    - To covert the whole surface with a fabric, which will help to smooth the surface and resemble a continuous surface

- To have a dense amount of variation points to create a smoother as possible surface

As it was decided to design a non-continuous surface the actuated points should be rounded ended cylinders or balls and be as close to each other as possible. If a fabric is used to smooth the surface and resemble a continuous surface it has to be elastic and very malleable to offer small resistance to the deformation.

- To be actuated by SMA
    - To integrate a recovery mechanism when the SMA colds

As SMA actuators produce work like a linear actuator, the design must integrate a way to connect the SMA to the cylinders or balls from previous condition. In the university department the method most used is to introduce the SMA through a hole in a screw and secure it with two nuts. Recovery mechanisms are normally a spring or a second SMA pulling in the opposite direction. As a SMA from above the surface cannot be implemented, a compression spring will be used as a recovery mechanism.

- To measure movements of the surface

For this requisite in the mechanical design it has to be taken into account the size of the sensor used (fig.25). Also it has to be devised the way to hold the sensor in position.

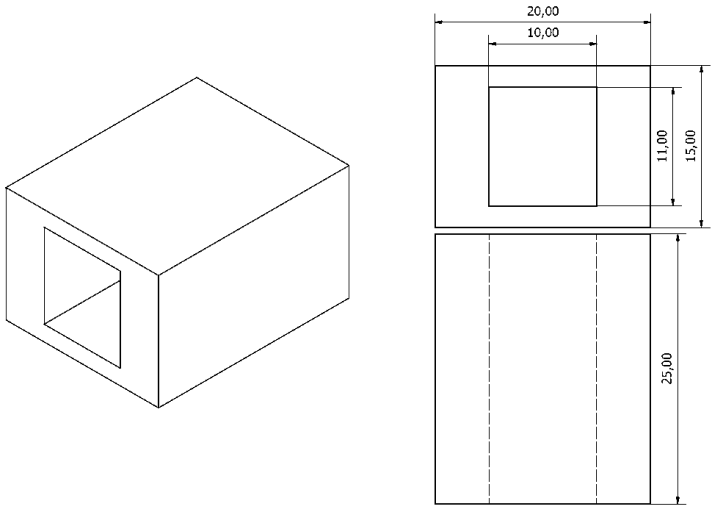


**Figure 25: Simplified Sensor Design**

### 5.1.3. Design

The basic model around the mechanical design is developed is to make it resemble to a table, which basic parts are the legs and a base. From the previous analysis it was concluded that is also needed to design the actuated points of the surface and the sensor's holder. As the base depends on the actuated points this was the first part designed.

- **Actuated points**

Since the beginning the actuated points were divided in two parts, the part that would be connected to the SMA actuator, named plastic cylinder, and the rounded part that would form the surface, rubber part. The names were given because the idea was to build the prototype using a 3D plastic printer but for the rounded part it was needed a softer material like rubber. That was also the reason for which the actuated points were divided into two parts.

  - **Plastic Cylinder**

The initial design of the plastic cylinder, fig. 26, was a 2cm diameter cylinder for the main body and 1cm diameter cylinder at both ends, also in this design it was included a kind of "rings" with the idea to use them to hold the spring (in this initial design it was thought to use a expansion spring). The longest end was designed to fit inside the rubber part and the shorter end had a through hole would had passed the SMA wire, the design was thought with the idea of clamping the SMA wire. This design was rejected because there could appear problems while printing the part as the bottom end cylinder was smaller than the main body and because the rings could not be strong enough to hold the spring, besides that the hole was so small that it would disappear while printing.

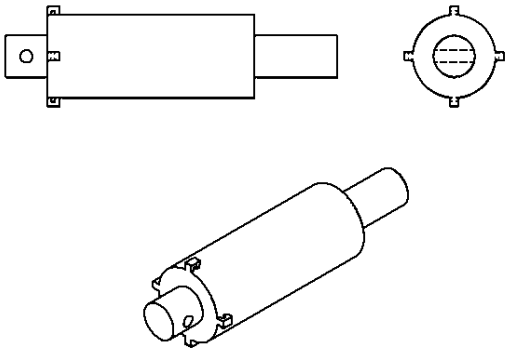

**Figure 26: Initial Plastic Cylinder Design**

For the following design the rings were taken off the design and they will be substituted by metallic arcs that would be inserted on the body, also de bottom end

cylinder became of the same diameter of the main body, which got slightly decreased (1.8cm diameter) due to tolerances needed as this part and the base were going to be 3D printed. Even though initially this was the final design after printing and testing it some changes had to be made to adjust the design.

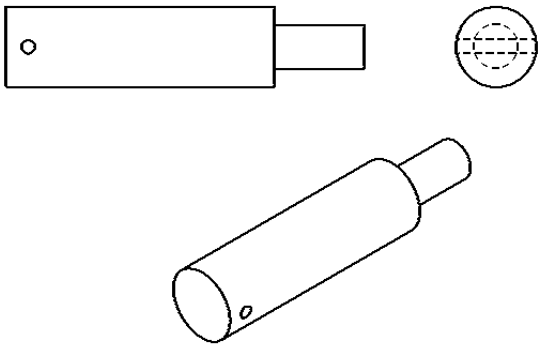

**Figure 27: First 3D Printed Plastic Cylinder Design**

In the final design the hole across the cylinder was removed, as the SMA wire was clamped with a screw and two nuts, a new hole at the bottom of 4mm and 2cm deep was introduced to clamp the SMA wire. Also at the top of the main body cylinder a small portion was suppressed to create a flat surface to which the magnet used for the sensor could be attached. Final dimensions and specifications can be observed on the following plane, fig. 28.

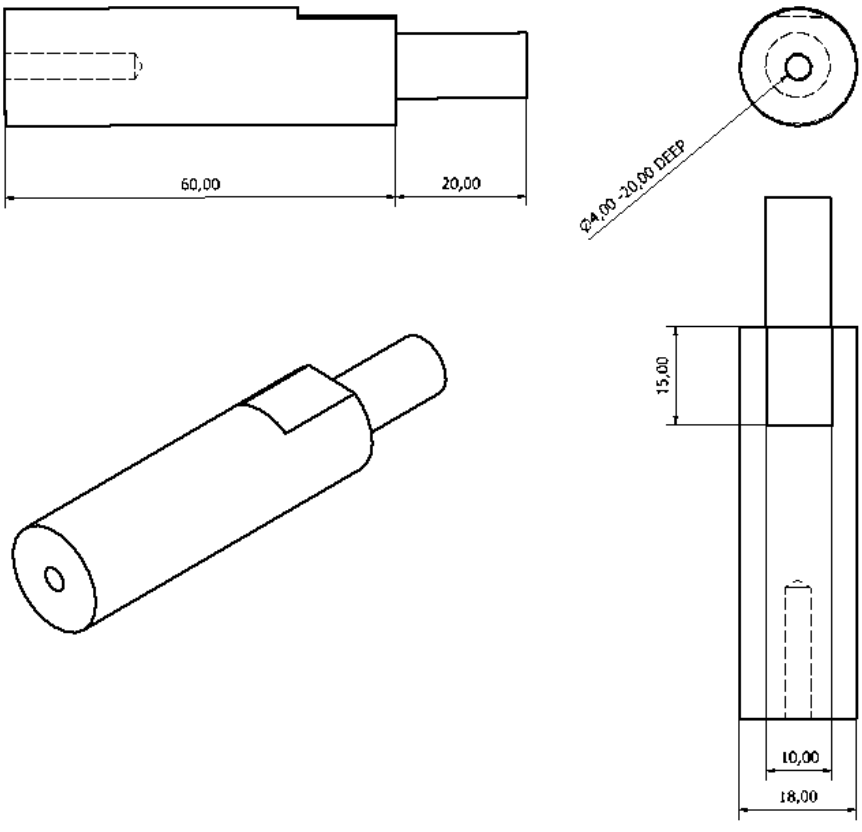


**Figure 28: Final Plastic Cylinder Design**

### ○ Rubber Part

The initial design of the rubber part was just a cylinder of 2cm diameter and 5cm length with a rounded end and a hole at the other end to fit on the plastic cylinder. This design was missing a way to hold the fabric that would cover the surface, that part was added later as a through hole along the main axis of the cylinder, with this hole the fabric could be locked to the actuated points. The last change introduced before the final design was the change of the cylinder diameter from 2 cm to 1.8cm as the plastic part had suffered this change for tolerance's needs. Final dimensions and specifications can be observed on the following plane, fig. 29.

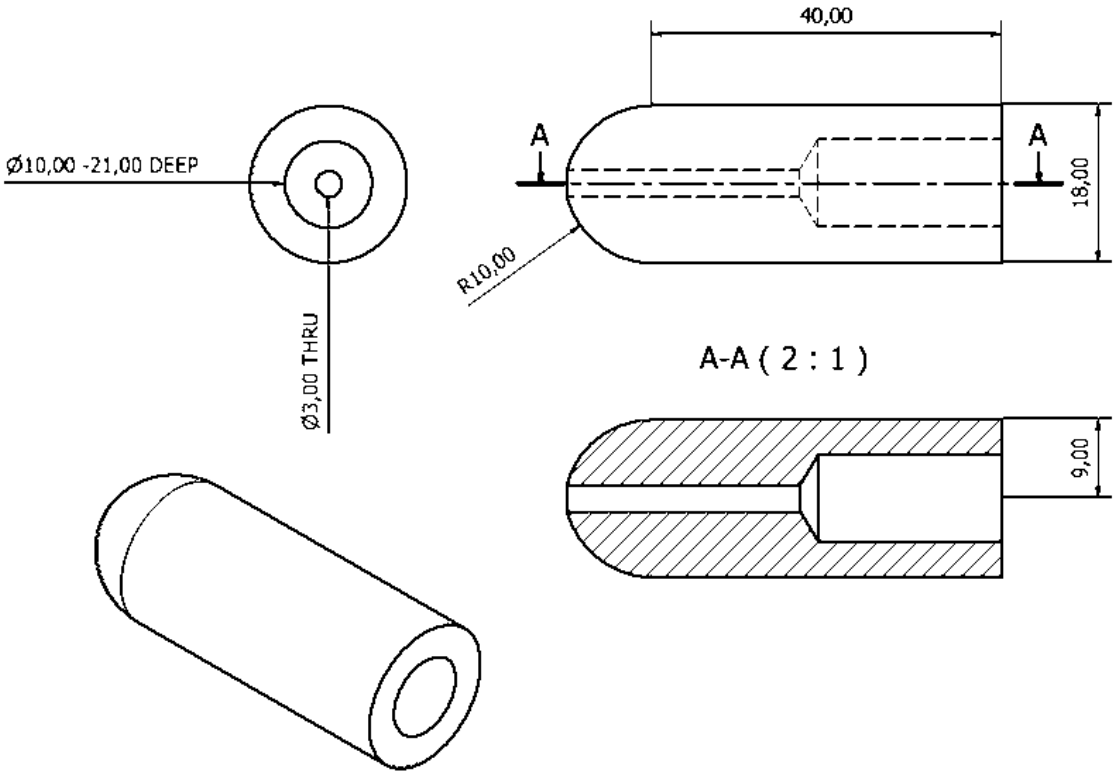


**Figure 29: Final Rubber Part Design**

- **Base**

The base was designed to be used as a rail for the actuated points and the idea was to put two bases parallel. The holes in the base are separated 0.5cm to create every 4 holes a gap between then in which the sensor and sensor holder for the interior plastic cylinders would fit. The base was designed to hold 16 plastic cylinders as this is the maximum number of signals allowed by the electronics board used for control.

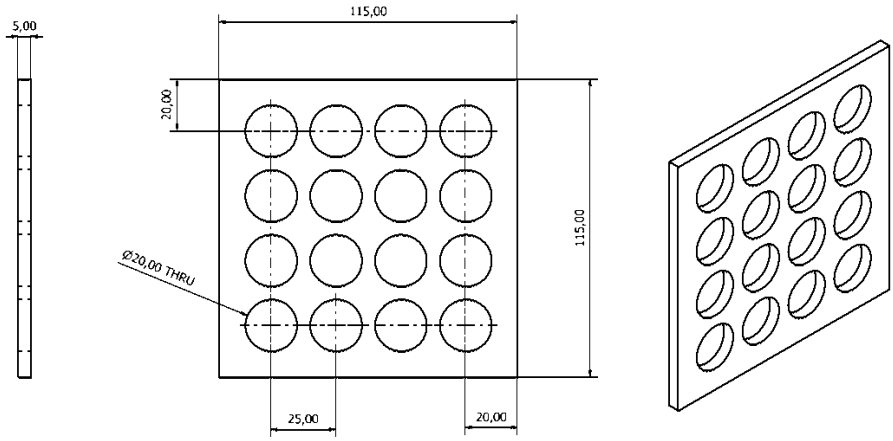


**Figure 30: Top Base Design**

Initially when spring used was to be an expansion one connected to the cylinder by the rings printed the lower base and the top one were going to be different with the idea of including 3D printed rings to hold the springs, this design can be observed in fig. 31. As expansion springs of the diameter needed cannot be found at stores, the lower base took the same design that the top one and compression springs would be used, these springs will be attached to the plastic cylinders and the base itself will be the limit for the spring as the holes are of a smaller diameter than spring's diameter.

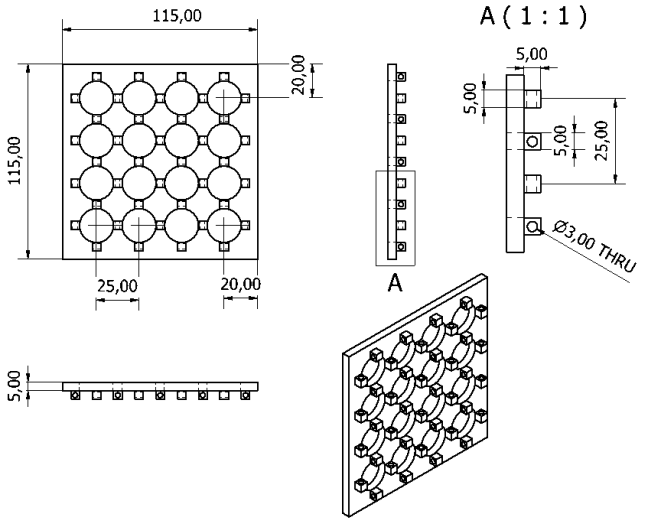


**Figure 31: Initial Lower Base Design**

- **Columns, legs and sensor holder**

The first idea was to 3D print these parts. But as the decided design was a $1cm^2$ square column with different lengths, as it was almost the space in the interior of the sensor and the idea was to keep the whole mechanical design as uniform as possible, to achieve a fast prototyped if the lengths needed to be adjusted these parts were finally built with a wood square strip of $1cm^2$. The columns will be used to separate the two bases two create a rail for the actuated points and the sensor holder will be located in that gap, therefore both will be the same length, 6cm; the legs will be used to separate the surface structure from the electronics and to provide enough space for the SMA wires, in this case the length is 10cm.

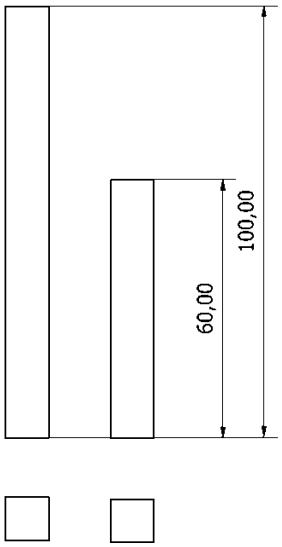


**Figure 32: Columns, Legs and Sensor Holder Design Annotated**

The sensor would be hold with double-sided tape and the columns and legs could be screw or glue to the base. The final method used to secure the columns and legs would be screw so the prototype can easily be taken apart.

- **Assembly Design**

Once all the parts were designed, the assembly design was built and some of the surfaces that could be achieved with the real model were simulated. These aspects can be observed on the following images.

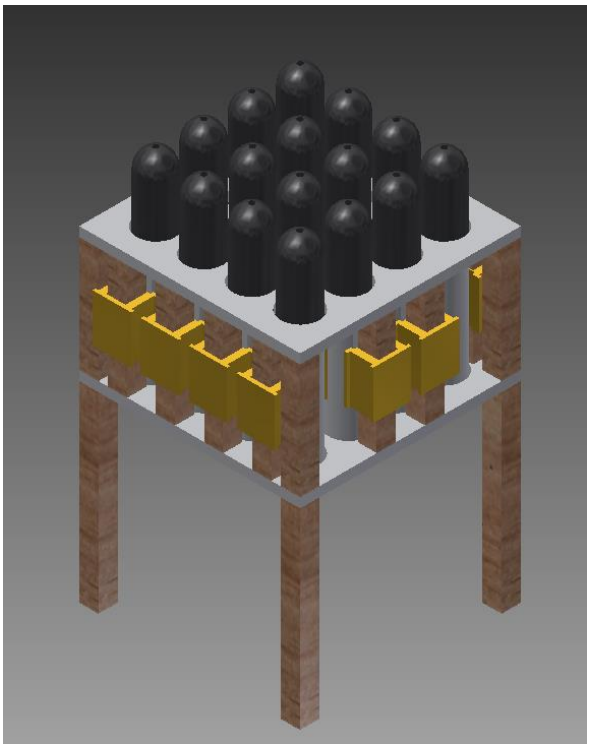

**Figure 33: Assembly Design**

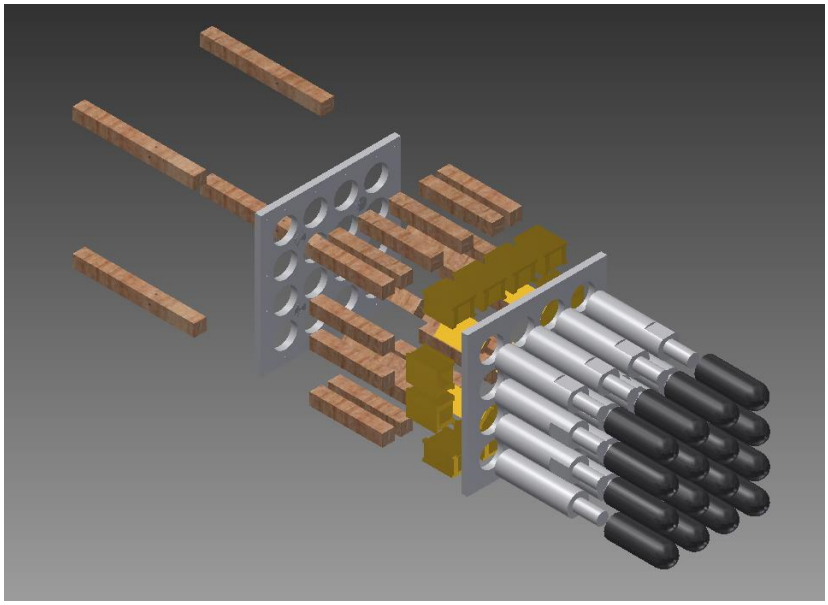

**Figure 34: Exploded View of the Assembly**

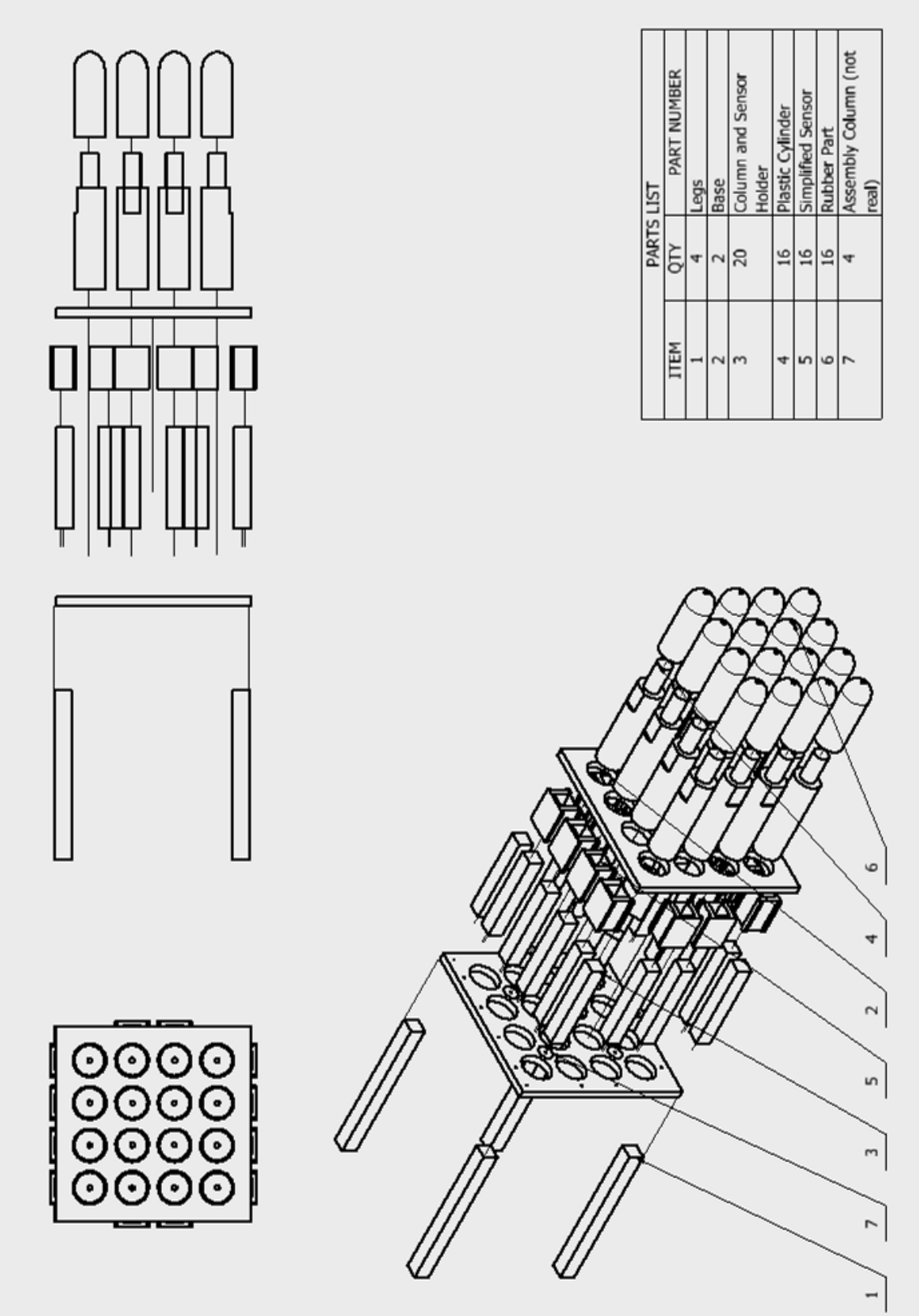


**Figure 35: Exploded View Drawing with BOM**

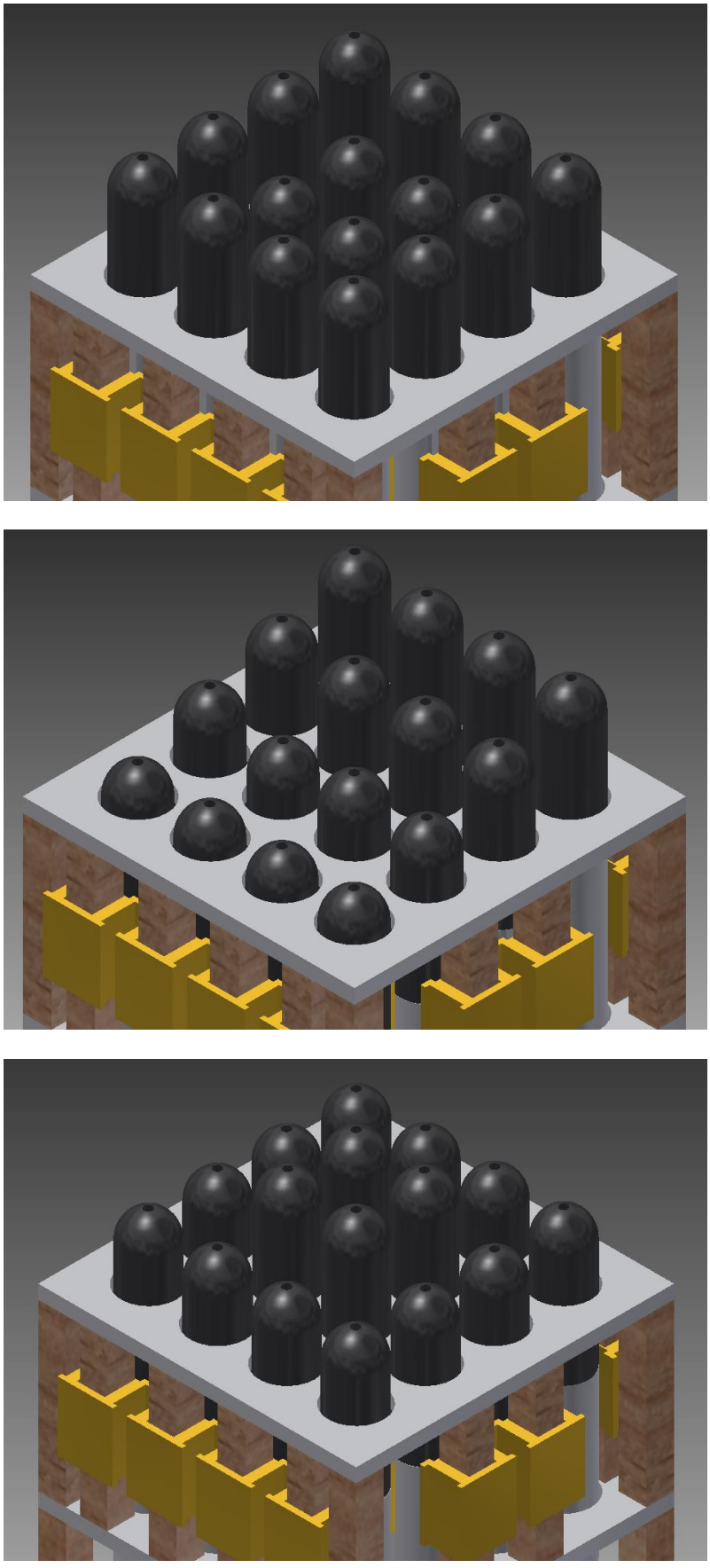

**Figure 36: Examples of Achievable Surfaces**

### 5.1.4. Implementation

In this phase all the parts were built and later assembled. Except the legs, columns and sensor holder, the parts were 3D printed in the university.

3D printers work by melting a material, in this case a plastic thread, and extruding it. While the extrusion process is realized the extruder is moved by motors in a Cartesian coordinate system, the movements are determined by a program that slice the design and that communicates with the 3D printer controller board.

In the slicer program one can configure extrusion speed, filling pattern, amount of solid slices at bottom and top… Also the heating temperature of the base and the extruder need to be adjusted depending on printing material, in this case the base was heated to 110℃ and the extruder was heated to 230℃ as ABS plastic was used.

This technology has been used as provides a fast and cheap way of prototyping compared with classical prototyping methods. As the whole printing process was realized on the university and as not a great amount of knowledge is needed to 3D print, this reduces costs of qualified personal and shipping costs. In addition to these advantages, there is the reduced cost of open hardware 3D printers that provide enough quality on finished products that most of the prototypes need during the first experimental tests. Other prototyping methods as CNC machines no only need qualified personal, which increases costs, but the machines used have higher costs.

On the following pages, the characteristics of each of the parts that composed the prototype are explained.

- **Base**

This part was printed twice as the same design was used as bottom and top bases. The holes that can be observed on fig. 38 were realized after printing using a threaded rod that had been heated previously.

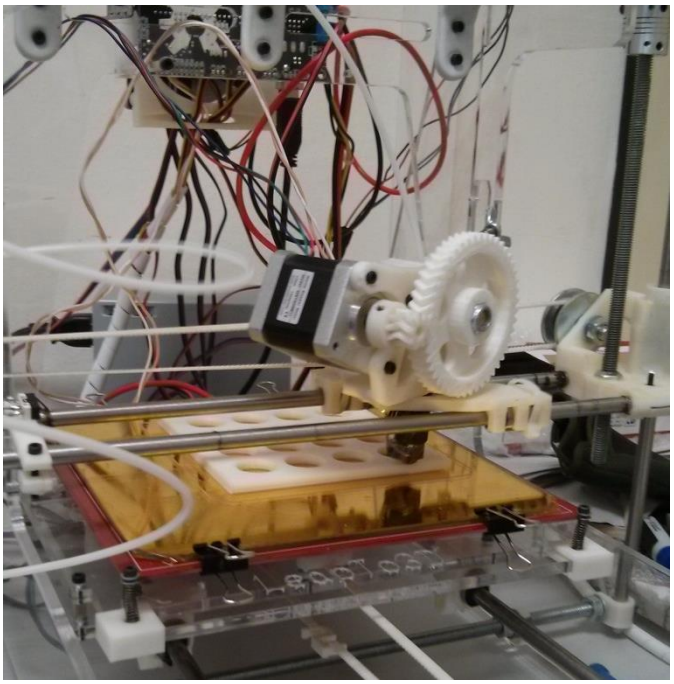

**Figure 37: 3D Printing the Base**

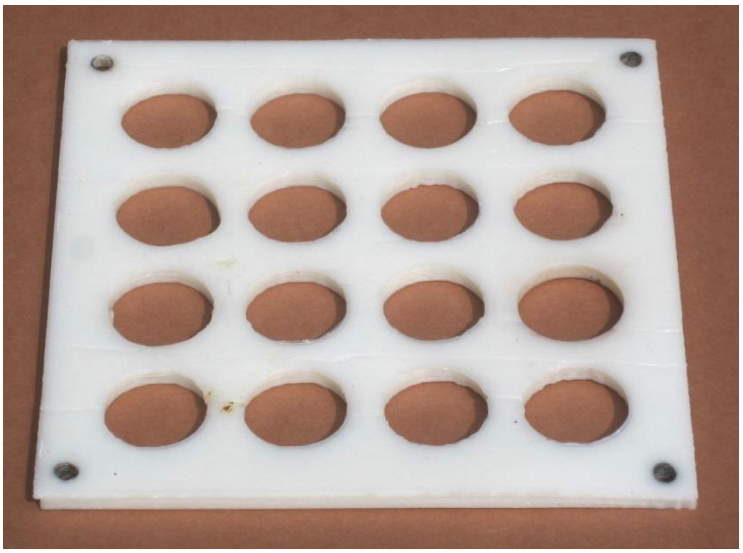

**Figure 38: One of the Two Bases Printed**

- **Rubber Part**

Even though this part should have been building with rubber as was designed for the prototype it was 3D printed as it is a faster mode to prototype.

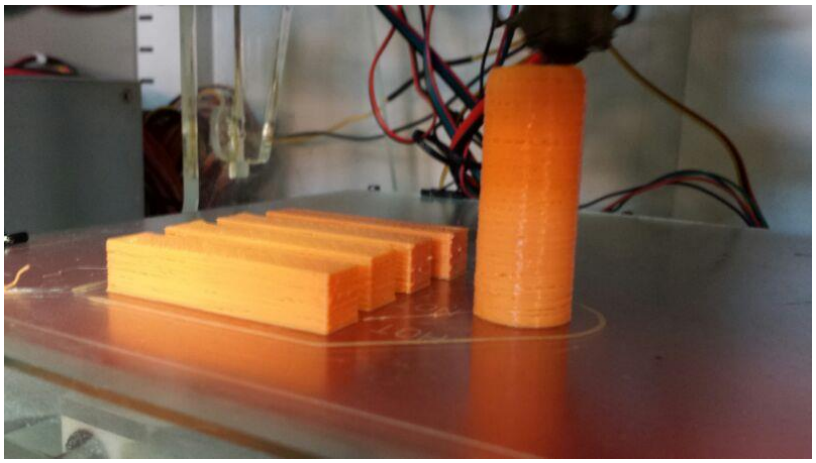

**Figure 39: 3D Printing a Rubber Part and Four Columns That Later Were Built with a Wood Strip**

**Figure 40: Rubber Part Printed**

The Rubber Part was covered with Teflon (PTFE) to reduce friction between the bases and the rubber part and the plastic cylinder.

- **Plastic Cylinder**

In this case the final design was developed after this phase as some changes were introduced due to a change in the way of attaching the SMA wire to the cylinder and to ease the attachment of the magnet strip, needed for the sensor. The design printed was the one that appear in fig. 27. Also as happened with the rubber part, this part was covered with Teflon (PTFE).

**Figure 41: Plastic Cylinder with Spring Attached and the Rubber Part**

- **Assembled Model**

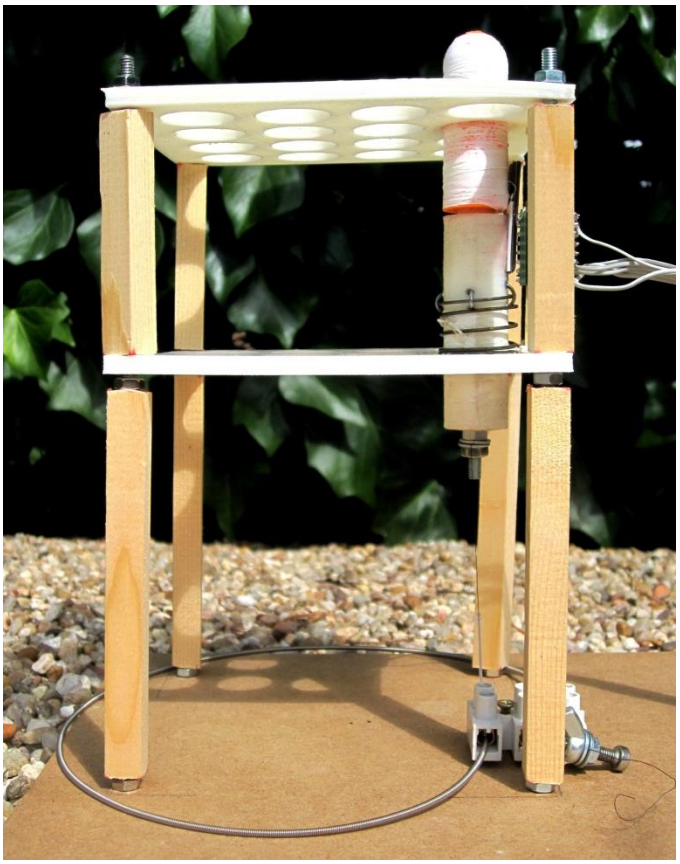

**Figure 42: Assembled Model with One Actuated Point**

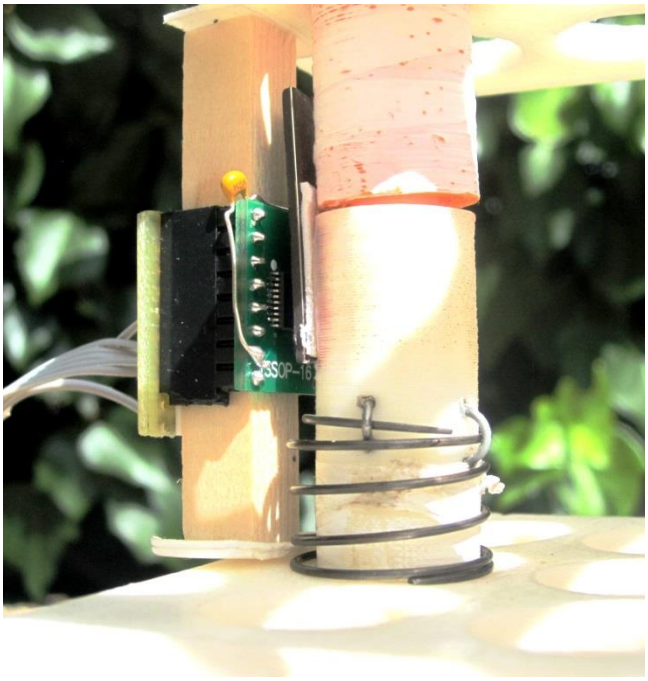

**Figure 43: Detailed View of Sensor and Actuated Point**

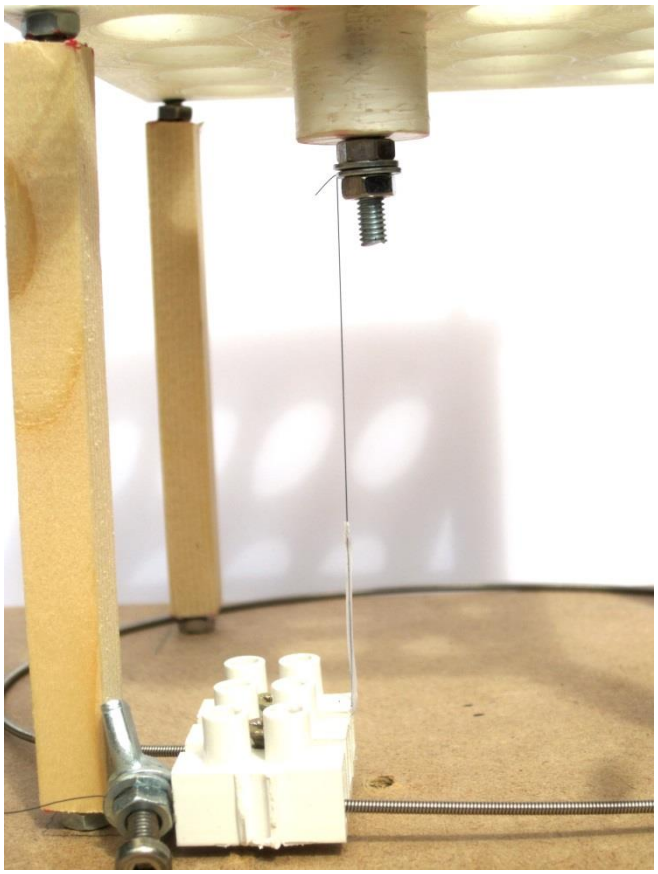

**Figure 44: Detailed View SMA Actuator Connected to the Plastic Cylinder**

As it can be observed on the figures above the prototype was completed with wood columns and a terminal block was used to lock the gimp and the SMA wire.

### 5.1.5. Testing

This phase was done while testing the surface control and it will be analyzed in the section “Experimental Measurements”.

## 5.2. SMA Drivers PCB Design

SMA actuators need to have a driver as the control signals are around 0,5A and the SMA need around 5A to work. In the department Antonio Flores had designed a driver’s board and hand built it for four SMA, but as the surface prototype could have until sixteen actuated points it was better to design a PCB instead of hand built the board for sixteen SMA.

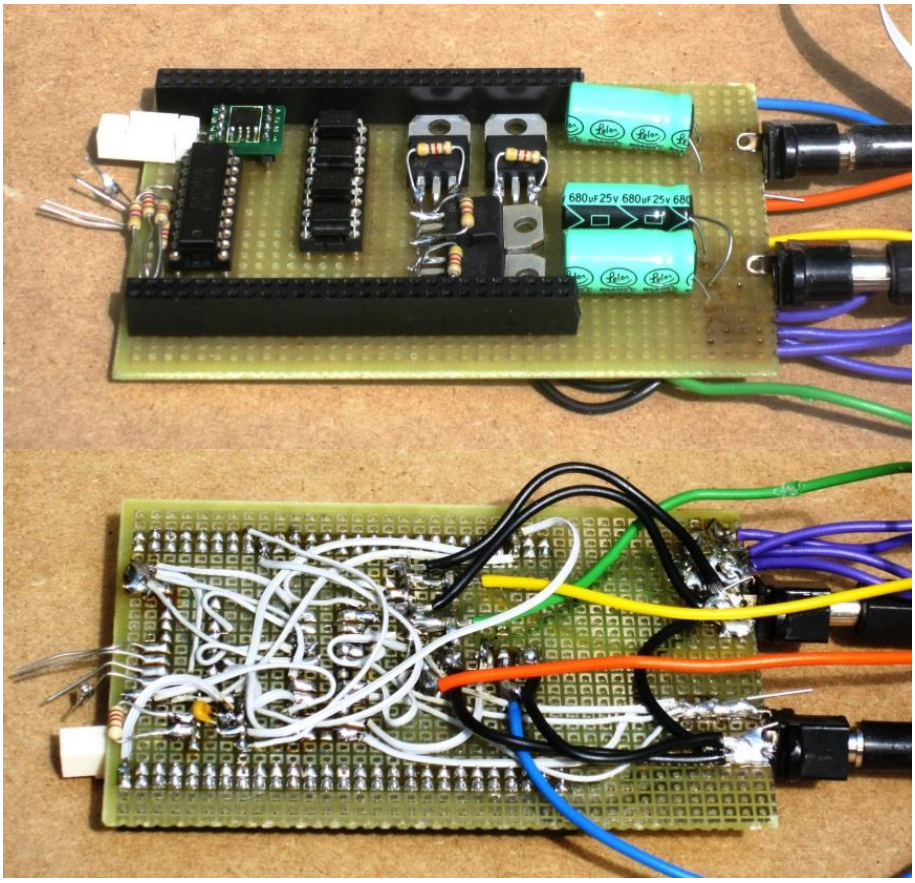


**Figure 45: Driver's Board Designed by Antonio Flores**

The tool used to design the schematic circuit and the PCB was OrCAD as it is the tool used for Antonio Flores, who was supervising the development of this part of the project. OrCAD is a Microsoft Windows proprietary software tool developed by Cadence Design Systems. It is used to create electronics schematics and electronics prints used while manufacturing printed circuit boards

The final schematic circuit, fig. 46, can be divided in four different parts:

1) The first part function is to receive the PWM inputs and by means of a voltage buffer to prevent interferences. This part is composed by a line of 16 female headers, a 5V source and two octal non-inverting buffers.

2) The second part is used to insulate the first part of the board from the high current part used to supply current to the SMA. This part is composed by sixteen opto-isolators and a voltage source that will be used later to supply the voltage needed for the MOSFETs.

3) The third part is used to supply the current needed to the SMA wires. This part is composed by sixteen blocks, one per SMA, that consist on a MOSFET to regulate the current, a resistor and the connectors for the SMA, this part also has its own voltage supply.

4) The fourth part was an addition to the circuit on fig. 45 with the idea of minimizing the number of connections to the control board. This part is composed by a 4-16 multiplexer and the same voltage source than the first part.

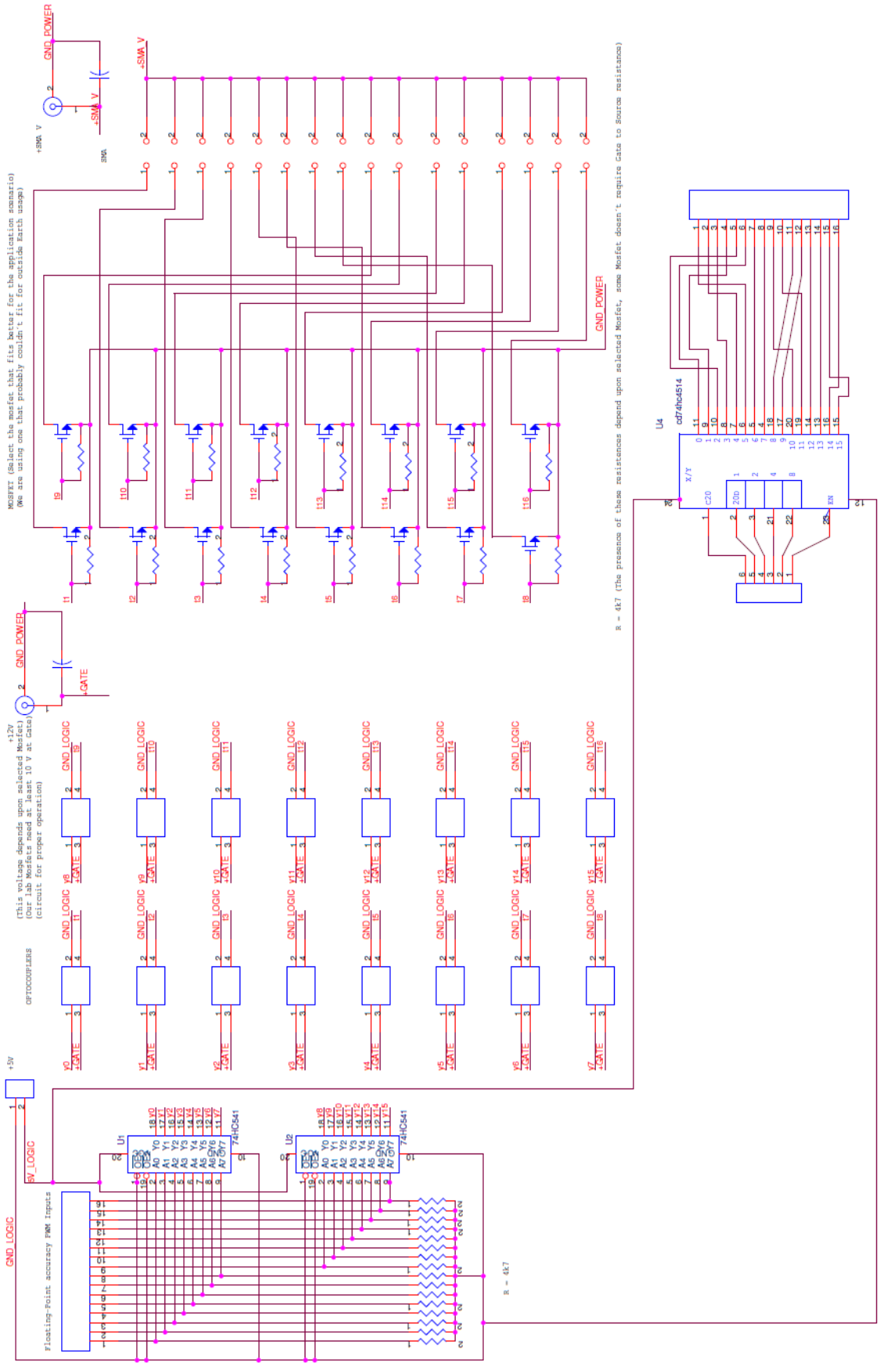

**Figure 46: SMA Driver's Schematic Circuit**

From the previous schematic it was generated the final PCB, this PCB had the requirements of being as small as possible and not to have any via. In fig. 47, the placement of the components and routes can be observed. The routes' widths are 35, 55 and 75 mils and these widths were assigned under the following criteria: regular routes, 5V source routes and SMA part of the circuit (third part) respectively.

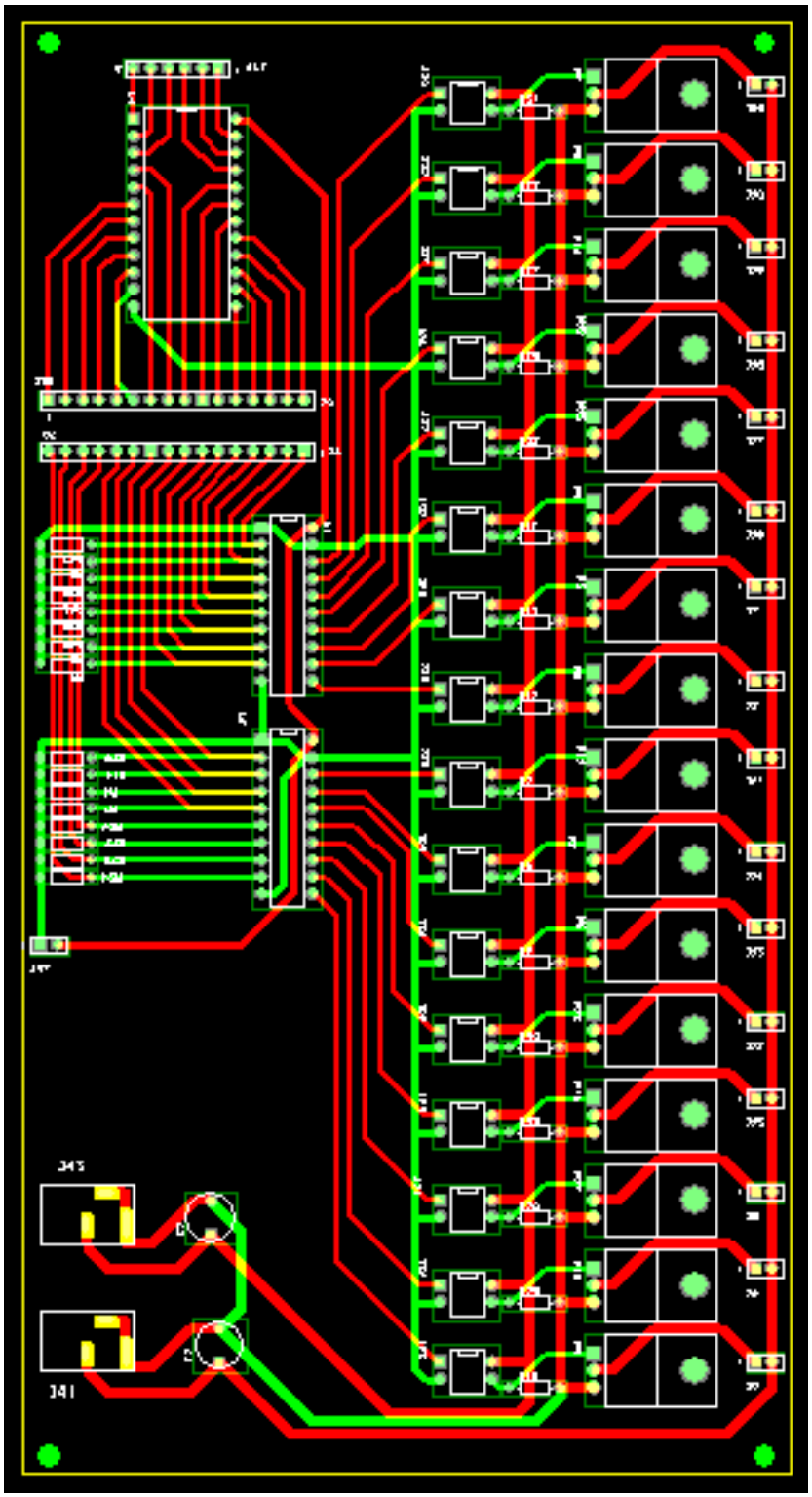

**Figure 47: SMA Drivers PCB**

## 5.3. SMA Position Control

On the state of art was explained how SMA actuators show hysteresis effects, these effects cause the actuator to be a non-lineal system. The problem that appears with non-lineal systems is to develop a simple controller that do not require high computational power and that can track the reference smoothly without presenting a big overshoot.

In this case the position controller used is based on the position controller used in the Department of Systems Engineering and Automation of the University Carlos III of Madrid developed by A. Villoslada, A. Flores-Caballero, D. Copaci, D. Blanco and L. Moreno, fig. 48. In that controller, the solution was implemented by a PD controller, which exhibited an undesirable overshoot and a steady error, and a Fuzzy Logic error compensator to attenuate the errors noted. Due to the prototype model it was added a small integrator, which as will be observed on the "Experimental Measurements" section resulted in minimal error.

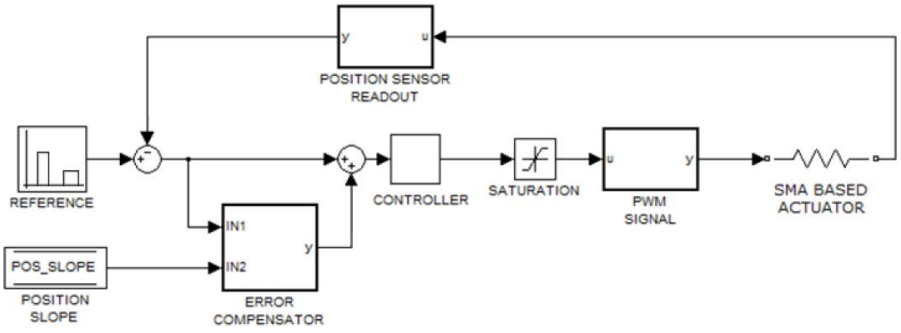


**Figure 48: Implemented Control Scheme by A.Villoslada, A. Flores-Caballero, D.Copaci, D. Blanco and L. Moreno**

One aspect that has to be evaluated is the resolution of the sensor used to measure the position because the error compensator will improve as the resolution of the sensor increases. Also some of the values that configure the Fuzzy Logic have to be changed in function of the resolution; in this case, the displacement Hall Effect sensor used has a resolution of approximately $0.48\mu m$.

The resolution of the sensor is also important as the prototype use thermal actuators. This is ought to the fact that the control will heat the SMA wire until the sensor receives a lecture just about the reference point, if the sensor has a poor resolution this lecture will be far from the reference point and therefor some oscillations will be produced. Also SMA wires present problems when they overheat and this will also be prevented with a high resolution sensor as the overheating above the reference point can be considered minimal.

## 5.4. Surface Control

To control the surface the board STM32F407VG, which integrates an ARM-Cortex-M4 32bits, has been used in conjunction with a Hall Effect sensor to measure the actuated points position.

Due to its complexity, the surface control has been developed using a program in Simulink developed by Antonio Flores to control in position and velocity SMA actuators, this control is achieved by two PID controllers, one for velocity and the other one for position. The control has been developed on Matlab using Simulink blocks as it is a fast prototyping method to program. Simulink is a graphical programming language tool that allows system's simulations and automatically generates source code to be used on other environments.

The surface control program is composed by two subprograms, one that it is installed on the board and another one that is run on a computer. These programs are conformed by regular Simulink blocks and by the blocks generated by Antonio Flores as part of his PhD. Thesis.

The program installed on the board, fig. 49, allows the board to acquire data sent by the computer through a USB port and to send to the computer the data required to know the position, velocity and sensor error. This program also interprets the data received to generate the PWM signals used to control the SMA.

The program that is run on the computer, also named host program and that can be observed on fig. 50, is used to send to the board the PID parameters and the velocity and position wished and to receive the values of the position, velocity and sensor error, among others. The parameters of the PID controllers were adjusted through a trial and error method and the final values for each PID were:

- PID Velocity Controller:
    - **Proportional:** 0.005
    - **Integral:** 0.008
    - **Derivative:** 0
    - **Feed-forward:** 1.1

- PID Position Controller:
    - **Proportional:** 0.8
    - **Integral**: 0.03
    - **Derivative:** 0.09
    - **Feed-forward**: 0

As the control wanted was in position, a constant value of velocity of 200 it was maintained and the position reference value it was varied between 0 and 5200.

The control explained was realized for one actuated points, in case of simulating the whole surface model with its 16 actuated points the programs of fig. 47 and 48 would have to be replicated 16 times changing the port of the board to which the PWM signal is send and the port where the sensor is connected.

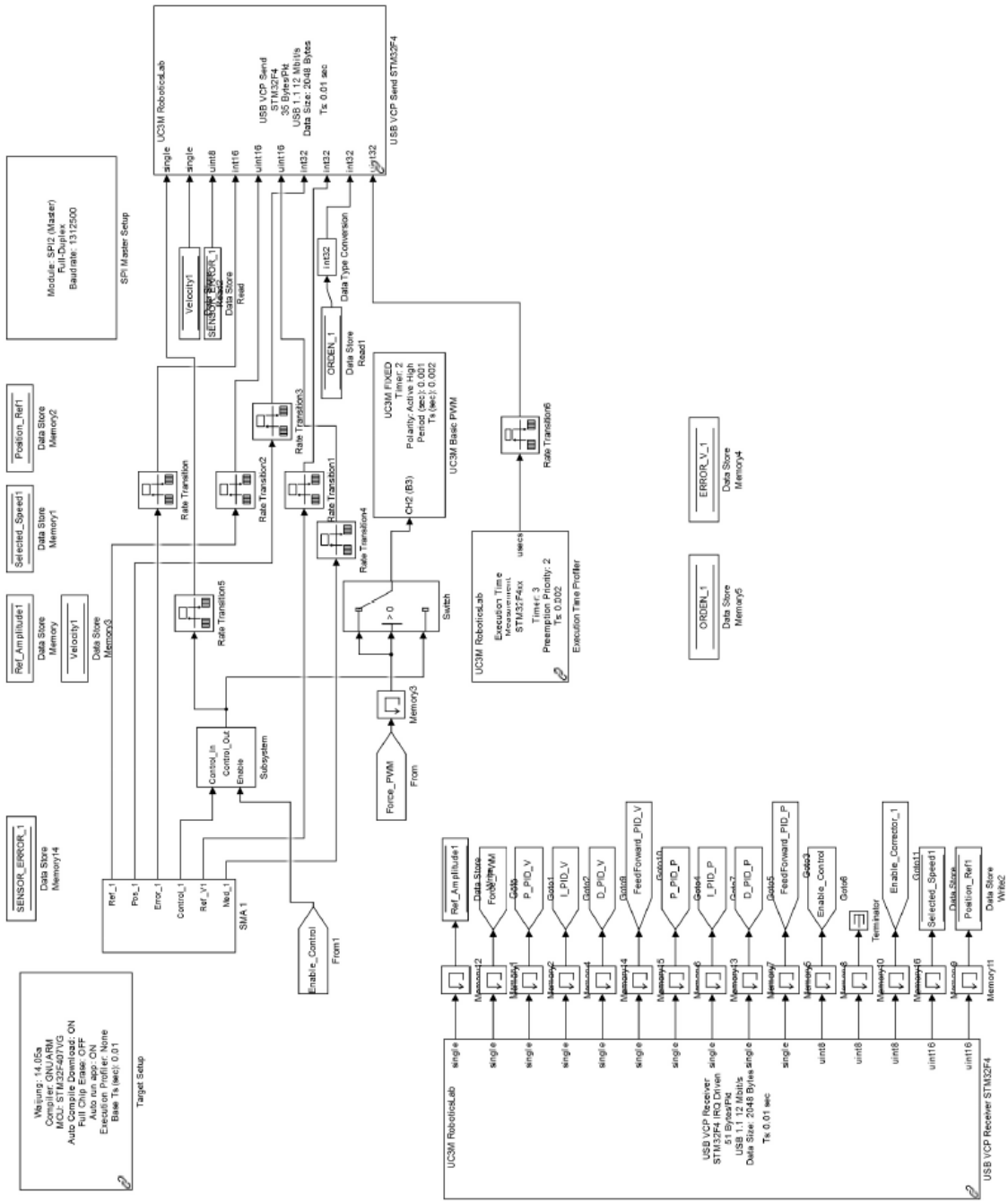

**Figure 49: Program Installed on the Board**

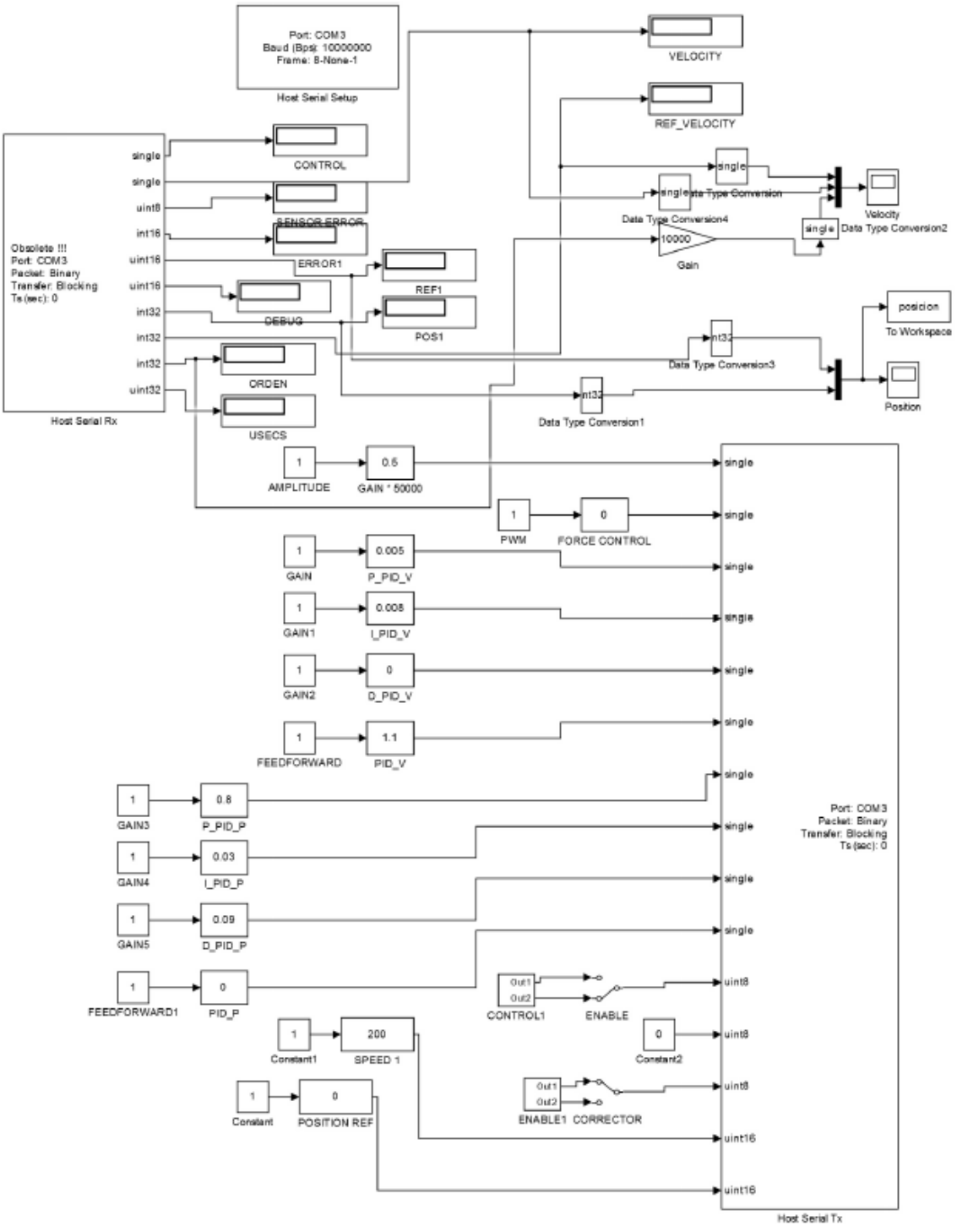


**Figure 50: Program Run on the Computer to Control the Surface**

# 6. Experimental Measurements

Once the prototype was built, the whole system was completed by a Nitinol wire of 0.15mm of diameter and by connecting the drivers' board to the SMA and the control board, to which was also connected the position sensor. In order to validate the design a prototype, a series of tests were needed to run.

The first tests were run to adjust the model determining the voltage source for the SMA and exact values introduced on the surface control program. The tests started with a voltage source of 12V; at this voltage the SMA did not received enough current and therefor it did not heat enough and position changes were minimal. The voltage was raised until, at a source voltage of 16V, the SMA contracted the range allowed by the spring. The complete model can be observed on the following image, fig. 51.

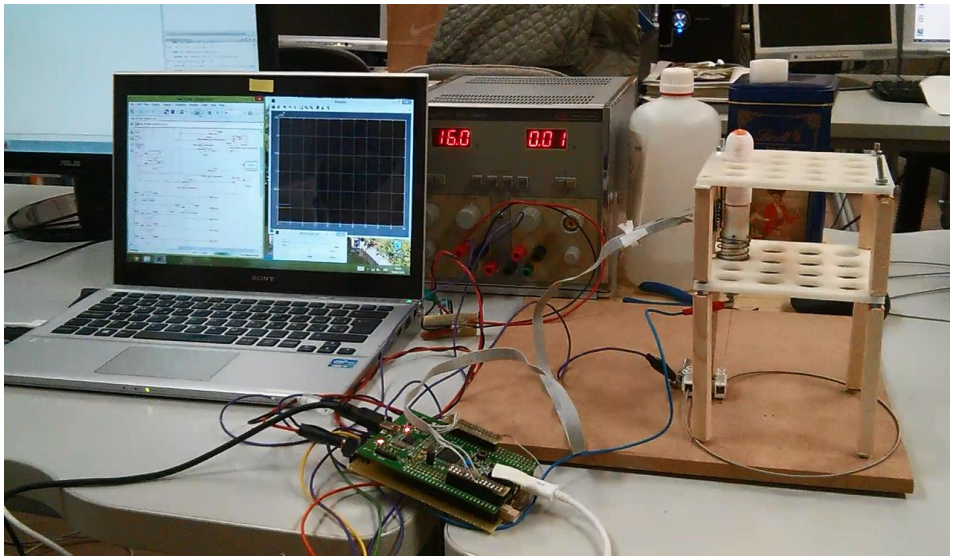

**Figure 51: Complete Model: Mechanical Prototype, Drivers' Board, Control Board, Sensor, Power Supply and Computer**

Once the surface control had been adjusted, different positions were set in a time series to collect data to study how the system was behaving. The data collected was time, position reference set and position read by the sensor. In this project no other data was needed as the goal was to control in position the actuated points of the surface.

The last test run was performed to compare the results obtained from the prototype with a simulated model. For this purpose, it was used the SMA model created on Simulink by Dorin Copaci, fig. 52, and the reference signals were the signals that had been collected during the previous test on the real prototype. This model uses a similar control algorithm than the prototype and it simulate the behavior of an

SMA wire as it heated to recover its initial length after being elongated plastically in cool. On the model the parameter related to the SMA and the velocity were needed to be adjusted to the following:

- **SMA diameter:** 0.15
- **Velocity:** 1, as it is the slowest one
- **Reference:** It was used the vector generated from the tests realized on the prototype.

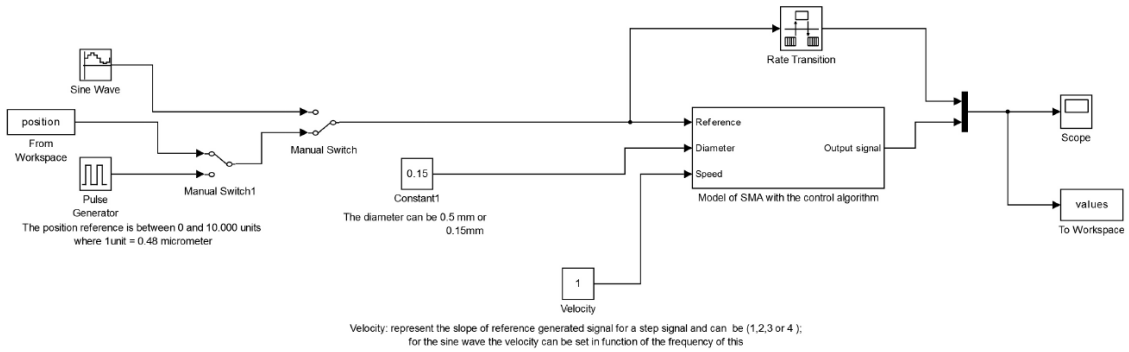


**Figure 52: SMA Simulink Model**

In the following two images we can observe how the position evolves as the reference point change over time. In figure 53, it is represented the data obtained with the SMA Simulink Model and, in figure 54, it is represented the real data obtained by exciting the SMA connected to the surface model.

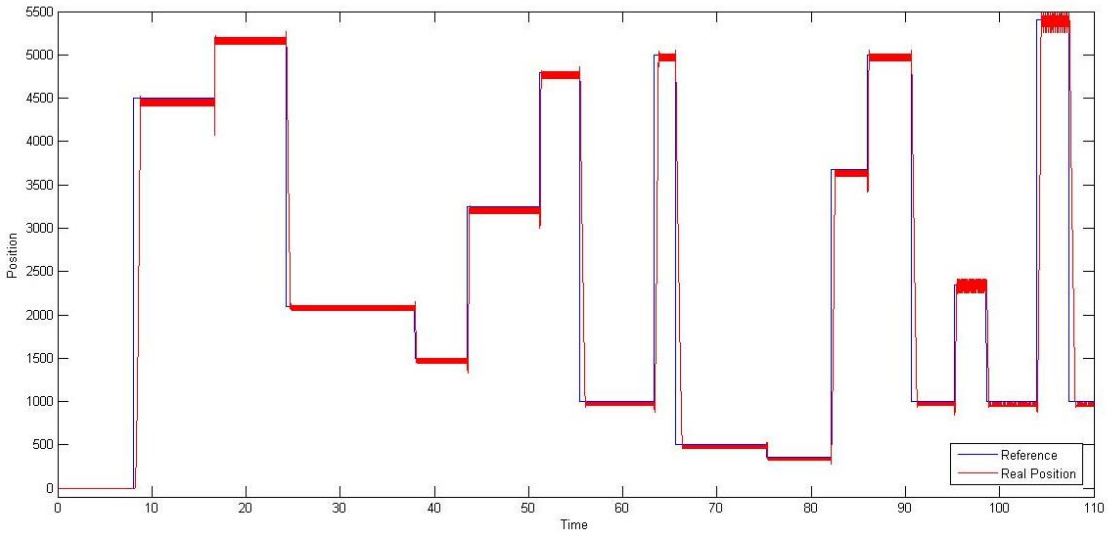


**Figure 53: SMA Simulink Model Position vs. Time Graph**

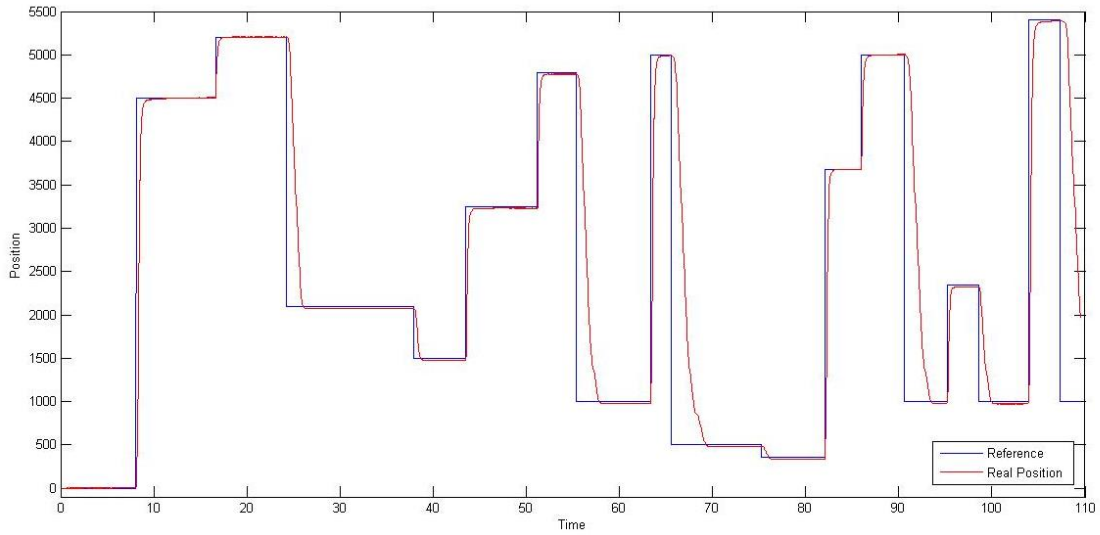


**Figure 54: Real Model Position vs. Time Graph**

Observing the graphs, it is obvious that the controller used on the real model is more adjusted and stable than the one used on the SMA Simulink model, that suffer oscillations and it present a visible steady error as the oscillations are produced under the reference point. On the other hand, the response time to reach a reference point higher than the actual one is higher on the real model than on the simulated. This aspect could be corrected by changing the PID parameters of the controller on the real model but it will have to be considered that decreasing the response time could

produce the system to start oscillating, as the simulated model. These aspects can be observed in a detailed view on fig. 55.

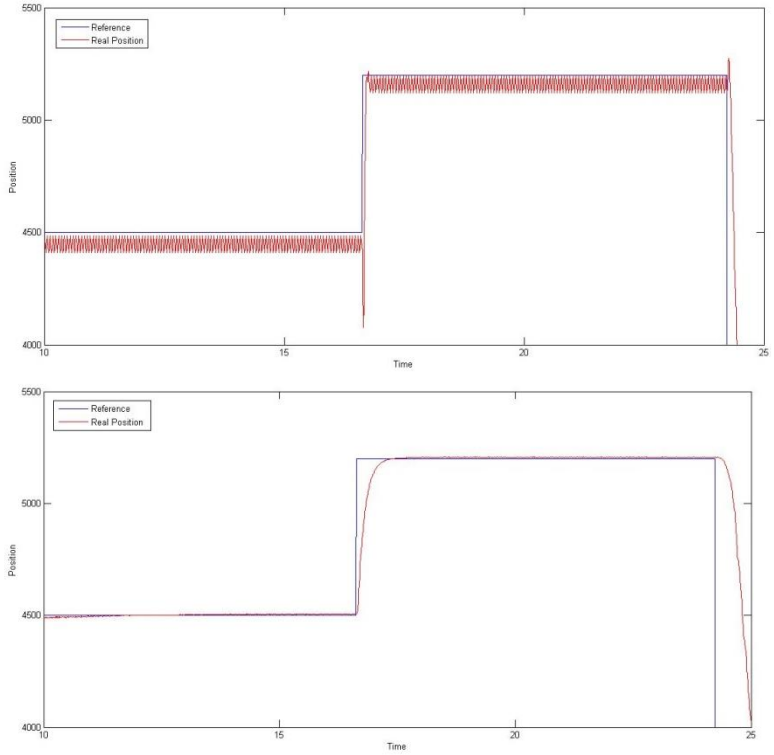


**Figure 55: Detail View of the Heating Response Time and, near Reference point, Oscillations and Steady Error. SMA Simulink Model (Up). Real Model (Down)**

Also the hysteresis that SMAs suffers it is higher on the real model than on the simulated model, this means that when the next reference point is lower than the actual one in the real model it takes more time to the SMA to cool and recover the length required, fig. 56. This last aspect could be affected as the tests were performed on July, so ought to the higher temperature in the lab the response time of the real model in colder room may be close to the simulated model.

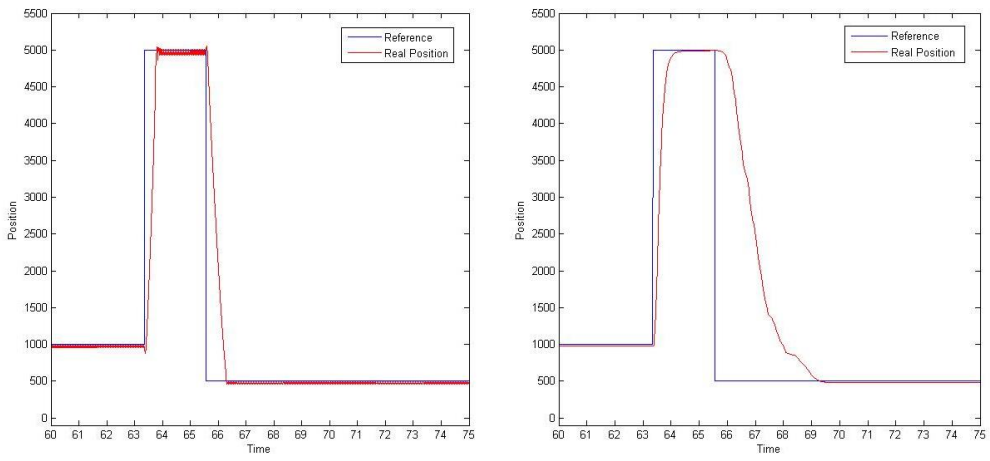


**Figure 56: Detail View of the Cooling Response Time. SMA Simulink Model (Left). Real Model (Right)**

In the following two images we can observe how the absolute error evolves over time. In figure 57, it is represented the data obtained with the SMA Simulink Model and, in figure 58, it is represented the real data obtained by exciting the SMA connected to the surface model

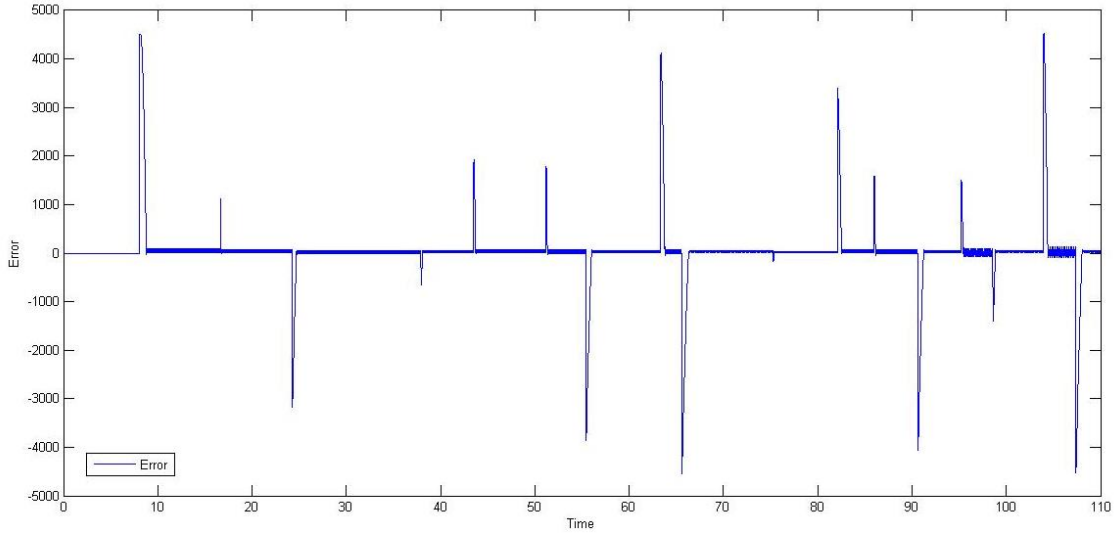


**Figure 57: SMA Simulink Model Error vs. Time**

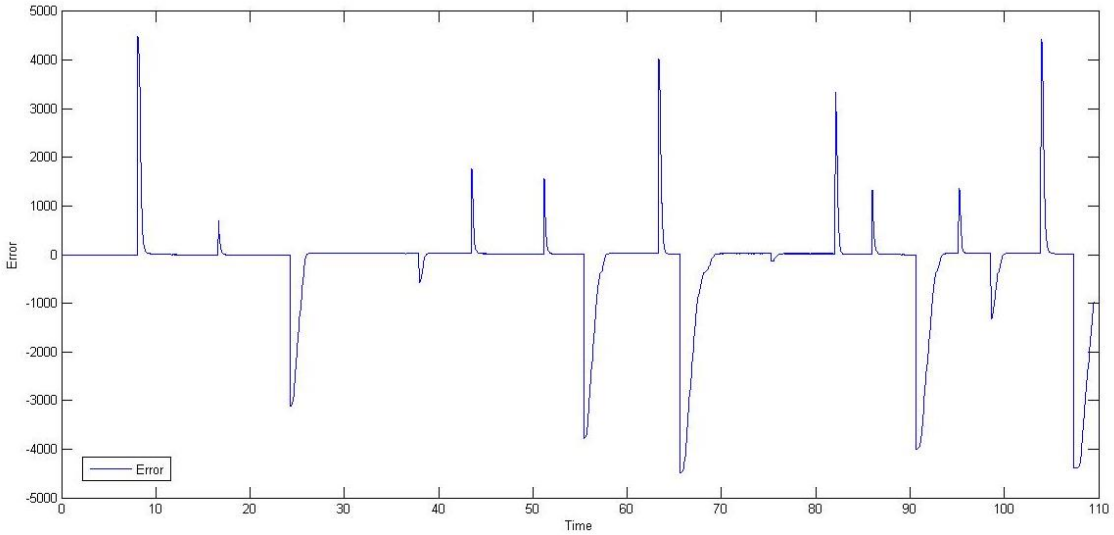


**Figure 58: Real Model Error vs. Time**

On the graphs can be observed that the simulated model presents oscillations, which were analyzed earlier, with an error near 0 of almost 100 units, and on the real model the error is much smaller and it cannot be observed at least a zoom is apply over the graph; in this case, it is observed a steady error up to 30 units on the worst cases and less than 5 units on oscillations.

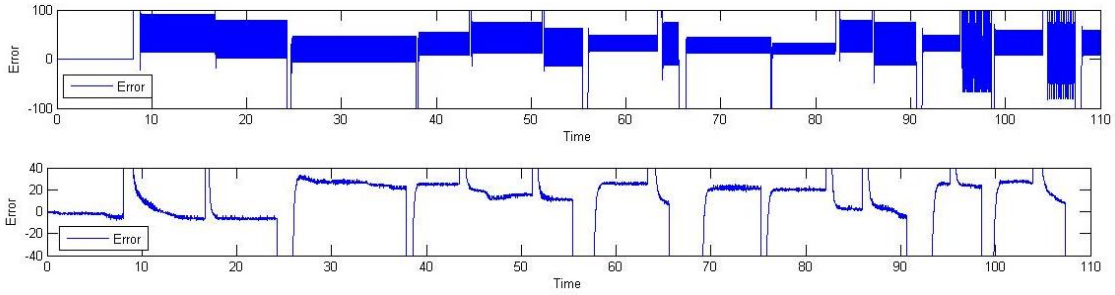


**Figure 59: Detailed View Error near 0. SMA Simulink Model (Up). Real Model (Down)**

# 7. Conclusion and Future Works

The goal of this project was to develop a morphing surface actuated with SMAs and control it in position to create different shapes. Also the surface needed to be continuous or have a high density of actuated points and it needs to be able to recover the initial shape, a flat surface. The other goal associated with the first one was to design a PCB for the SMA driver's board that could be used later in other projects using SMA actuators.

After studying the state of art of SMA actuators and surfaces morphing, it was detected that surfaces morphing using SMA actuators has been researched mostly for airplanes and all the devices are based on non-continuous surfaces covered by a continuous adaptable layer. Moreover, in one of the possible areas of application of this project, anti-bedsores' surfaces in which the need of a continuous surface is more important, most of the devices are based on mats filled with compressed air or liquids and are actuated with motors, compressors and valves. The surface designed was a non-continuous surface with the highest possible density of rounded actuated points, the size of the sensors was the limiting factor, as creating a continuous surface would have produce higher errors due to cooling velocity and due to strains between different actuators of the surface.

While developing the project some problems were detected on the mechanical design and corrected in the final prototype, these were detailed explained in the respective section. The section of SMA driver's design was the section that took more time to be completed as it was the first PCB designed and the process of self-learning to use OrCAD was the longest process. The surface control section did not present relevant problems beyond getting familiarized with the Simulink blocks and control developed on the university.

In the last phase of the project the prototype was tested and compared with the simulations realized for a standard SMA wire of the same diameter and length. With these tests it was validated the adjustment of the controller parameters and the prototype reaction as even though response times were higher on the real model that on the simulation the system was more stable and it present a smaller steady error and oscillations. Also as an anti-bedsores' surface there does not exist the need of a small response time since it is recommended smoother changes to which the person will not react unwittingly.

Once the project was concluded and due to the results obtained during the tests some new projects could arise and evolve from this one, some of this could be:

- Using the sixteen actuated points develop a graphical interface to control the surface, this could also lead to a phone app in which different patterns of movement could be set. As a result, the surface shape would change along the time without the need of introducing new values to change the position of each of the actuated points.

- Another project could be to calculate and build a prototype of a seat that can be used by a person. With this project it could be developed an anti-bedsores' surface less noisy than the actual ones that use motors and compressors.

- Also it could be developed a mechanism similar to the one developed on the MIT, fig. 20 and 21, to represent objects and interact remotely with real objects.

In the last two projects different position sensors should be used to be able to increase the density of actuated points and to ease building phase and any repairs needed.

# 8. Budget

Project's Duration: 12 ECTS (360 hours)

| | Qty | Unit Price | Subtotal | Grand Total |
|---|---|---|---|---|
| **Labor Cost** | | | | **3,600.00€** |
| Documentation | 60 h | 10.00€ | 600.00€ | |
| Prototype's Design | 70 h | 10.00€ | 700.00€ | |
| SMA Driver's PCB | 100 h | 10.00€ | 1,000.00€ | |
| Prototype's Assembly | 20 h | 10.00€ | 200.00€ | |
| Surface Control | 30 h | 10.00€ | 300.00€ | |
| Experimental Tests | 20 h | 10.00€ | 200.00€ | |
| Thesis writing | 60 h | 10.00€ | 600.00€ | |
| **Material Cost** | | | | **381.75€** |
| Prototype | | | | 84.60€ |
| SMA Wire | 8 m | 6.00€ | 48.00€ | |
| Teflon Lining | 8 m | 0.65€ | 5.20€ | |
| Gimp | 8 m | 0.80€ | 6.40€ | |
| Mounting elements (wood columns and base, screws and nuts) | 1 | 5.00€ | 5.00€ | |
| 3D printing | 1 | 20.00€ | 20.00€ | |
| Hardware | | | | 297.15€ |
| STM32F407VG Board | 1 | 15.00€ | 15.00€ | |
| SMA Driver's PCB | 1 | 30.00€ | 30.00€ | |
| Optocouplers K1010 | 16 | 0.20€ | 3.20€ | |
| Transistors STP310N10F7 | 16 | 4.65€ | 74.40€ | |
| Decoder 4 to 16 | 1 | 2.43€ | 2.43€ | |
| 74HC541 | 2 | 1.06€ | 2.12€ | |
| AMS 5311 Sensor and magnet | 16 | 10.00€ | 160.00€ | |
| Other Electronics Elements | 1 | 10.00€ | 10.00€ | |
| Software | | | | 0.00€ |
| Matlab 2013 | 1 | 0.00€ | 0.00€ | |
| Autodesk Inventor Professional 2014 | 1 | 0.00€ | 0.00€ | |
| Orcad Capture 9.2 | 1 | 0.00€ | 0.00€ | |
| **Research and Development Total** | | | | **3,981.75€** |

# 9. Bibliography

[1] Mohd Jani, J., Leary, M., Subic, A., & Gibson, M. A. (2014). A review of shape memory alloy research, applications and opportunities. Materials & Design, 56, 1078-1113.

[2] Machado, L. G., & Savi, M. A. (2003). Medical applications of shape memory alloys. *Brazilian Journal of Medical and Biological Research*, *36*(6), 683-691.

[3] Mavroidis, C., Pfeiffer, C., & Mosley, M. (2000). 5.1 conventional actuators, shape memory alloys, and electrorheological fluids. *Automation, miniature robotics, and sensors for nondestructive testing and evaluation*, *4*, 189.

[4] Falvo, A. (2007). Thermo mechanical characterization of nickel-titanium shape memory alloys. *Doctoral Course on Mechanical Engineering*, 1-128.

[5] Van Humbeeck, J. (1999). Non-medical applications of shape memory alloys.*Materials Science and Engineering: A*, *273*, 134-148.

[6] Sofla, A. Y. N., Meguid, S. A., Tan, K. T., & Yeo, W. K. (2010). Shape morphing of aircraft wing: Status and challenges. *Materials & Design*, *31*(3), 1284-1292.

[7] Barbarino, S., Bilgen, O., Ajaj, R. M., Friswell, M. I., & Inman, D. J. (2011). A review of morphing aircraft. *Journal of Intelligent Material Systems and Structures*, *22*(9), 823-877.

[8] Follmer, S., Leithinger, D., Olwal, A., Hogge, A., & Ishii, H. (2013, October). inFORM: dynamic physical affordances and constraints through shape and object actuation. In *UIST* (pp. 417-426).

[9] Flores-Caballero, A., Copaci, D., Blanco, M. D., Moreno, L., Herrán, J., Fernández, I., ... & Grande, H. (2014). Innovative pressure sensor platform and its integration with an end-user application. *Sensors*, *14*(6), 10273-10291.

[10] Vasina, M., Solc, F., & Hoder, K. (2003, December). Shape memory alloys-unconventional actuators. In *Industrial Technology, 2003 IEEE International Conference on* (Vol. 1, pp. 190-193). IEEE.

[11] Lee, S. Y., Chwa, K. Y., Hahn, J., & Shin, S. Y. (1994, May). Image morphing using deformable surfaces. In *Computer Animation'94., Proceedings of* (pp. 31-39). IEEE.

[12] Calkins, F. T., & Mabe, J. H. (2010). Shape memory alloy based morphing aerostructures. *Journal of Mechanical Design*, *132*(11), 111012.

[13] Kadkhodaei, M., Salimi, M., Rajapakse, R. K. N. D., & Mahzoon, M. (2007). Microplane modelling of shape memory alloys. *Physica Scripta*, *2007*(T129), 329.

[14] Martín Clemente, A. I. (2013). Modelado y control de sistemas no lineales de tipo SMA.

[15] Huang, W. (2002). On the selection of shape memory alloys for actuators.*Materials & design*, *23*(1), 11-19.

[16] Stirling, L., Yu, C. H., Miller, J., Hawkes, E., Wood, R., Goldfield, E., & Nagpal, R. (2011). Applicability of shape memory alloy wire for an active, soft orthotic.*Journal of materials engineering and performance*, *20*(4-5), 658-662.

[17] Sawyer, P. N., Page, M., Baseliust, L., McCool, C., Lester, E., Stanczewski, B., ... & Ramasamy, N. (1976). Further study of nitinol wire as contractile artificial muscle for an artificial heart. *Cardiovascular diseases*, *3*(1), 65.

[18] Bellini, A., Colli, M., & Dragoni, E. (2009). Mechatronic design of a shape memory alloy actuator for automotive tumble flaps: a case study. *Industrial Electronics, IEEE Transactions on*, *56*(7), 2644-2656.

[19] Cano Sánchez, A. (2010). Estudio e implementación de actuadores basados en aleaciones SMA.

[20] Villoslada Peciña, Á. (2010). Diseño y aplicación de un actuador SMA en el control de manos robóticas.

[21] Flores, A., Copaci, D., Martin, A., Blanco, D., Moreno, L. (2012) Smooth and Accurate control of multiple Shape Memory Alloys based actuators via low cost embedded hardware. *International Conference on Intelligent Robots and Systems. IROS 2012*

[22] Autodesk, Inc. (2011). *Imagine Design Create*. New York: Melcher Media.

[23] Cong, R. *Muscle Wire: Motor-less Mechanical Motion*. Retrieved September 13, 2014, from Jameco.com: http://www.jameco.com/jameco/workshop/productnews/musclewire.html

[24] Drugs.com. *Bedsores (Decubitus Ulcers).* Retrieved September 14, 2014, from Drugs.com: http://www.drugs.com/health-guide/bedsores-decubitus-ulcers.html

[25] Mayo Clinic Staff (March 25, 2014). Bedsores (pressure sores). Retrieved September 14, 2014, from Mayoclinic.org: http://www.mayoclinic.org/diseases-conditions/bedsores/basics/definition/con-20030848

[26] NASA (December 14, 2001). *Like a Bird's Wing*. Retrieved September 14, 2014, from Nasa.gov: http://www.hq.nasa.gov/office/aero/news/vol2_iss6/bird.htm

[27] Gilmore, C. (2014). *Materials Science and Engineering Properties, SI Edition*. Cengage Learning.

[28] Lala, D., Dumont, F. S., Leblond, J., Houghton, P. E., & Noreau, L. (2014). The Impact of Pressure Ulcers on Individuals Living with a Spinal Cord Injury. *Archives of physical medicine and rehabilitation*.